1975

Prediction of Plant-,Soil- and Air-Temperature on a Microscale in the Desert

L. R. Martinez

I. Dirmhirn

1973 PROGRESS REPORT
[FINAL]

PREDICTION OF PLANT-, SOIL- AND AIR-TEMPERATURE ON A MICROSCALE IN THE DESERT

L. R. Martinez and I. Dirmhirn (Project Leader)
Utah State University

US/IBP DESERT BIOME
RESEARCH MEMORANDUM 75-45

in

REPORTS OF 1974 PROGRESS
Volume 3: Process Studies
Abiotic Section, pp. 49-68

1973 Proposal No. 2.3.5.1

Printed 1975

Citation format: Author(s). 1975. Title.
US/IBP Desert Biome Res. Memo. 75-45.
Utah State Univ., Logan. 19 pp.

Ecology Center, Utah State University, Logan, Utah, 84322

ABSTRACT

The heat exchange during dry conditions in Curlew Valley for selected clear days was determined from recordings in 10-minute intervals. The two heat budget components, radiative exchange and heat flow in the soil, were studied in detail. Maximum surface temperature due to radiative exchange above, assuming no heat loss by other components, was determined and reduction of surface temperature by heat conduction into the ground was calculated as a second step to solve the heat budget equation. Substantial heat flow throughout a day was restricted to the upper 10 cm of the soil. Diffusivity of the soil was determined from soil temperature using phase and amplitude equations, of which the first gave better results.

INTRODUCTION

This study is concerned with the determination of radiative and conductive heat exchange of a cold desert. Curlew Valley was selected since the sagebrush desert type is one of the most extensive vegetation types in the United States and the study of this desert type has a high priority in the US/IBP Desert Biome program.

The movement of heat within the system is important in the analysis of the sagebrush ecosystem since the soil-plant interface forms a particular environment where climatic phenomena and processes occur and where, under normal circumstances, considerable exchange of heat occurs.

The thermal phenomena occurring in the air layer near the ground depend on the algebraic sum of all heat balance components: 1) influx and loss of heat by radiation at the surface (R_N); 2) heat exchange between the surface and deeper layers of the soil (Q); 3) heat exchange between soil and air (H); and 4) heat lost by evaporation of water from the surface or heat gained by condensation and sublimation of water vapor (LE).

In accordance with the law of conservation of energy, the inflow and outflow of heat in the active surface should be equal at any given moment. To express this condition mathematically, the algebraic sum of all inflow and outflow on the active surface is equal to zero:

$$R_N + Q + H + LE = 0 \qquad (1)$$

Of all the heat balance components mentioned above, only R_N and Q will be considered in this report, while H and LE will be part of a forthcoming study. From the existing data, days under "dry" conditions were selected so that LE could be considered zero. The equation then reduces to the first three components and a balance can be written considering H as a residual component while R_N and Q are studied in detail using the recorded data.

Net Radiation

The radiation balance or net radiation can be expressed by the equation:

$$R_N = (R_S + R_D)(1 - a) - R_E + R_A \qquad (2)$$

The radiant energy from the sun (0.3-4 μ) is dissipated and distributed by components of the earth's atmosphere as it passes downward toward the earth. A portion is reflected by clouds into outer space; some is absorbed by the molecules of carbon dioxide, oxygen, ozone and water vapor. Part is scattered and diffused by the molecules and small particles in the air. A portion of this diffused radiation is returned to outer space. The remainder is transmitted to the earth's surface as sky radiation (R_D). That fraction of the solar radiation that is not affected by the earth's atmosphere reaches the surface as a direct beam (R_S).

The global radiation reaching the earth's surface is partitioned into reflected radiation $a(R_S + R_D)$ and absorbed energy, which is utilized in heating the soil and the air above the soil, in latent heat of evaporation or in net long-wave radiation ($R_A - R_E$). Long-wave radiation (4-100 μ) is emitted by the earth's surface to the sky. It is referred to as "terrestrial" or "outgoing" radiation (R_E) and is equal to $\varepsilon \sigma \cdot T^4$. R_E takes place both day and night. Approximately 90% of this radiation is absorbed by the earth's atmosphere, primarily by water vapor. There is considerable reradiation of this absorbed radiation back to the surface. This is known as atmospheric radiation (R_A) which plays the major role in preventing excessive cooling at the earth's surface at night.

The difference between the outgoing terrestrial radiation and the atmospheric radiation is referred to as net long-wave radiation ($R_A - R_E$). At night R_S, R_D and $a(R_S + R_D)$ are zero, then

$$R_N = R_A - R_E \qquad (3)$$

Heat Flux Between the Surface and Deeper Layers of the Soil

The heat flux into the soil and the daily, seasonal and yearly heat accumulations are determined by the thermal properties of the soil and boundary conditions of the soil. These thermal properties or parameters are: K, λ and C_V. The following relationship exists between these three quantities:

$$\lambda = (K/C_V) \qquad (4)$$

The flow of heat in the soil can be described by the following equation:

$$(\partial T/\partial t) = \lambda \ (\partial^2 T/\partial Z^2) = (K/C_V)(\partial^2 T/\partial Z^2) \qquad (5)$$

The thermal diffusivity of the soil is of great importance as it governs the soil temperature distribution at different

depths. In soils with a low thermal diffusivity the daily and annual temperature amplitudes are smaller than in soils with higher thermal diffusivity.

OBJECTIVES

The objectives of this study are to:

1. Evaluate existing models to describe radiative and conductive heat exchange.
2. Determine the conductive and radiative properties of a cold desert.

REVIEW OF LITERATURE

In the last 40 years numerous workers have studied the seasonal and diurnal variation of radiative properties on vegetative surfaces as part of field studies of environmental aspects of land use. Many relationships between air temperature and solar radiation with soil temperature have been reported and several techniques have been used to study these relationships. A series of case studies showing the temperature response of the soil in several typical weather situations has been prepared and analyzed to show quantitatively the temperature change in the soil as a result of a given change on the external meteorological conditions.

Wexler (1936) pointed out that the net outgoing radiation decreases as the ground cools and reaches zero at a certain critical difference between air and ground temperature. Groen (1947) showed that the soil surface temperature approaches its minimum value asymptotically as the net radiation decreases to a minimum. The boundary condition used by Groen requires that, as the minimum ground surface temperature is approached, the net outgoing radiation and the heat flux through the ground surface approach zero. This requires that the vertical temperature gradient at the ground surface also approaches zero; it follows that the temperature can remain constant for only a shallow depth and a short period of time.

Fleagle (1950) shows that the lowest temperature a radiating surface may reach depends upon the thickness of the ground surface layer which undergoes temperature change, the conductivity of the layer and the presence of obstructions above the plane of the horizon.

Robinson (1947) found that the emission from short turf was close to black-body radiation at the minimum turf temperature. Houghton (1958) inferred from radiometer measurements in aircraft that the effective radiative temperature of open country at night lay between the temperature of grass minimum and screen air temperature. Analysis of solar and net radiation records on clear days at Rothamsted showed that the diurnal variation of net long-wave exchange was closely related to changes in surface temperature and that surface heating was proportional to net radiation (Monteith and Szeicz 1961).

Monteith (1959) studied the diurnal variations of soil heat flux under grass, potatoes and wheat. He reported that approximately 20% of the net incoming radiation was stored in the soil between 6 a.m. and 6 p.m. in the summer season under English conditions. The net radiation day was longer than the heat flux day. Mack (1969) reported that total solar radiation and resulting soil temperature had little correlation during a five-day period in Canada.

Hanks et al. (1971) developed a computer model to predict the temperature fluctuation in the subsoil from the temperature variation at the soil surface, taking into account changes in the apparent thermal conductivity with depth below the soil surface and soil temperature. They suggested solving equation 5 with a numerical approximation as follows:

$$(T_{i,j} - T_{i,j-1})/\Delta t = [(T_{i-1,j} - T_{i,j})\lambda_{i-\frac{1}{2},j} -$$

$$(T_{i,j} - T_{i+1,j})\lambda_{i+\frac{1}{2},j}]/\Delta Z^2$$

They reported that computed and measured soil temperatures agreed within 1.0 C when soil thermal diffusivity was assumed constant at 0.20 $cm^2 \cdot min^{-1}$. They also reported that where the thermal diffusivity was assumed uniform at .45 $cm^2 \cdot min^{-1}$, temperature errors grew from 1.0-1.7 C after three days to 1.7-3.1 C after six days.

Hanks and Jacobs (1971) indicated that, in comparing soil heat flow as estimated by the calorimetric, flux meter and a combination of the two methods, the best method for measuring daily soil heat flow is the calorimetric method in which soil temperature measurements are made to 64 cm for daily flux. They reported that the calorimetric method has the advantage of less critical assumptions than the flux meter for daily measurements with no accumulation of errors when integrated values over one day, or part of one day, are desired, and the combination method had the disadvantages of both methods.

Hanks et al. (1961) studied the relationship of net radiation, soil temperature and soil surface conditions on evaporation and reported that there was no direct relationship between net radiation or soil temperature and evaporation under the conditions of the experiment. This was probably due to the great limiting influence of soil moisture within the soil after the surface dries. Taylor (1928), working in Egypt, reported that no relationship between air and soil temperature could be traced. Many investigators (Antonova 1929, Hursh 1948, Brown 1943 and Reeder 1920) have reported the density of vegetative cover to have a significant effect on soil temperature. They have also found that the temperature of bare soil in summer was higher than that of a grass cover. Hide (1942) reported that the surface soil has a much higher variability than either air or deep soil temperatures. Austin (1972) reported about 15 C maxima difference between exposed and shaded points in the cold desert of Curlew Valley, Utah-Idaho. He found a strong correlation between hourly air temperature and soil temperature at 2-cm depth and between global radiation and soil temperature.

A computer model for the radiative heat exchange developed by Dirmhirn (unpublished) was written in a FORTRAN program (see Appendix A) and was used to determine the heat applied by radiation to the soil surface. In this model a thin soil layer was used as reference layer and as mass for the energy provided by the net radiation on clear days during the summer season. This method shows the heating of a surface layer by radiative processes when no other heat dissipation (exchange with the air or soil and evaporative processes) takes place.

LIST OF SYMBOLS AND DEFINITION OF TERMS

R_N = net radiation (cal. cm^{-2} min^{-1})

R_S = direct radiation (short wave radiation) (cal. cm^{-2} min^{-1})

R_D = diffuse and scattering radiation (short wave radiation) (cal. cm^{-2} min^{-1})

α = albedo (dimensionless)

R_E = emitted radiation of the active surface (long wave radiation) (cal. cm^{-2} min^{-1})

R_A = incoming radiation of the atmosphere (long wave radiation) (cal. cm^{-2} min^{-1})

R_S+R_D = global radiation (short wave radiation) (cal. cm^{-2} min^{-1})

R_A-R_E = long wave net radiation (long wave radiation) (cal. cm^{-2} min^{-1})

ε = emissivity (dimensionless)

σ = Stefan-Boltzmann constant (8.13×10^{-11} ly. $min.^{-1}$ K^{-4})

T = absolute temperature at the surface (degrees Kelvin)

K = coefficient of thermal conductivity of soil (cal. cm^{-1} $°C^{-1}$ min^{-1})

λ = coefficient of thermal diffusivity of soil (cm^2 min^{-1})

c = specific heat of soil (cal. $°C^{-1}$ g^{-1})

ρ_b = bulk density of soil (g. cm^{-3})

C_v = $c.\rho_b$ = product of specific heat and bulk density (cal. cm^{-3} $°C^{-1}$)

t = time (min.)

$\partial T/\partial t$ = change in temperature at a given point with time (°C. min^{-1})

$\partial^2 T/\partial Z^2$ = rate of change of temperature gradient ($°C^2$. cm^{-2})

Z = depth (cm.)

Δ = finite increment

i = subscript denoting the "ith" depth increment at i.Z depth

j = subscript denoting the "jht" time increment at a time j.T

a = empirical constant (0.820)

b = empirical constant (0.250)

c = empirical constant (0.094)

e = vapor pressure (mb.)

D = amplitude or phase equation (cm^2 $sec.^{-1}$)

A_1 = amplitude at Z_1 (°C)

A_2 = amplitude at Z_2 (°C)

δt = time interval between occurrence of maximum soil temperature at depths Z_1 and Z_2.

w = radial frequency

ΔHC = change in heat content

GENERAL DESCRIPTION OF EXPERIMENTAL AREA

Curlew Valley is a drainage basin astride the Utah-Idaho border encompassing some 3471 km^2. It is bordered by mountains ranging up to 2743 m above sea level on the east, north and west, and terminates at its southern end on the salt flats of the Great Salt Lake and the lake itself.

The valley floor is a lacustrine basin sloping from about 1280-m altitude at the lake level to 1585 m in the north in a series of step-like levels. This altitudinal gradient correlates with rainfall, soil and biotic gradients. Total annual precipitation ranges from 15 to 20 cm at the southern end of the valley to 36 to 41 cm at the northern end. From south to north, soil salinity declines from the very high levels of the lake fringe while soil organic matter increases progressively. The correlated vegetation gradient is formed by pickleweed (*Allenrolfia occidentalis*) which occupies a virtual monotype on the salt flats, greasewood (*Sarcobatus vermiculatus*) at an elevation close to the water table, shadscale (*Atriplex confertifolia*) on soil of substantial salinity, and big sage (*Artemisia tridentata*).

A study area was selected in a natural stand of sagebrush and a micrometeorological station was set up on this site. In general, the climate of the big sagebrush zone can be classified as "cold desert" with an average annual rainfall from 20 to 41 cm with about three-fourths of this occurring between October and May. Big sage is the principal primary producer species involved in the area and exhibits a season of observable growth between late March and early July, varying between years with the available moisture and with the prevailing temperature regime. The dominant texture of the soil appears to be silt loam.

METHODS

Instrumentation

Net radiation was measured with a net radiometer (Kahlisco) which was mounted on a stand about 1 m high above ground. Careful consideration was taken to ensure that the surface below the radiation balance meter was representative of a wide area of the surroundings.

Incoming solar and scattered radiation were measured with a star pyranometer placed over a rigid stand of 1-m height with a horizontal top surface. The site for the star pyranometer was free from any obstructions above the plane of the sensing element.

Copper-constantan thermocouples, as described by Dike (1958), were constructed to measure air temperature, surface temperature and soil temperature. Measurements of air temperature were made in the air immediately above the surface by means of unshielded thermocouples, which were installed on a triangular television tower about 8 m high. The thermocouples for the temperature measurements in the air were built from thin, 0.005-cm diameter copper and constantan wire. The heat dissipation from these thermocouples under natural environmental conditions is large

enough that no over-heating by radiative processes can occur. Thermocouples were placed on a triangular television tower at 5, 20, 50, 100, 200, 400 and 800 cm above the ground to measure air temperature. One more thermocouple was placed at 5 cm in the shade of a plant.

The surface temperature was measured by placing a surface thermojunction on the ground covered by a minute layer of dust. This surface junction was built from 0.1 mm Cu/0.12 mm constantan wire. A reference junction was placed at 125-cm depth.

Measurements of soil temperature were made at depths of 2, 10, 25, 50 and 125 cm. The thermocouple junctions were of 1-mm diameter gauge thermo wire. The thermocouple junctions were coated with an insulating paint to protect and insulate the junctions.

A Metrodata magnetic tape recorder was employed as a recording system. This digital recorder is designed for receiving data in time intervals from 1 sec to 1 hr. Intervals of 10 min were used throughout this study.

Procedure

Short-wave solar and scattered radiation flux ($R_S + R_D$), net radiation flux (R_N), surface temperature, subsoil and air temperature data as observed in the field were analyzed for several clear days during the summer season. Short-wave reflected radiation data were determined from incoming solar and scattered by considering albedo to be 0.16 as reported by Dirmhirn (1972). The diurnal variation in the net long-wave term ($R_A - R_E$) was calculated by difference (residual method) from formula 2. To determine the atmospheric radiation, the expression developed by Angstrom (Sellers 1965) was used:

$$R_A = \varepsilon \sigma T^4 (a - b \cdot 10^{-ce}) \qquad (7)$$

The values for the empirical constants (a, b and c) were taken from Geiger (Sellers 1965). The surface emissivity was assumed to be 0.9 (Sellers 1965). To obtain e, the vapor pressure of air, published data from Salt Lake City (National Weather Service FCST DFC, 1973) on air temperature, wet bulb temperature and atmospheric pressure were used together with psychrometric data from Smithsonian Meteorological Tables (1968).

Surface temperature, atmospheric radiation and emitted radiation from the surface of the soil were predicted with the model for the radiative heat exchange, to determine the heat applied by radiation to the soil surface. In this model, data of incoming solar radiation of several days during the months of June, July and August in Logan, Utah, were used.

A simulated profile subsoil temperature was predicted using the computer model developed by Hanks et al. (1971). Predicted soil temperatures were compared with soil temperatures observed in the field at 2-, 10-, 25- and 50-cm depths below the surface of the soil.

The initial temperature as a function of the depth and the surface temperature as a function of time used in the model were obtained from the soil temperature record in the field. The apparent thermal diffusivity values (equation 4) were also obtained from the soil temperature record in the field using phase and amplitude relations. The equations used to estimate the apparent thermal diffusivity from observed temperature variations at several soil depths were the amplitude equation:

$$D = (w/2)[(Z_2 - Z_1)^2 \ln A_1/A_2] \qquad (8)$$

and phase equation:

$$D = (1/2w)[(Z_2 - Z_1)/\delta t]^2 \qquad (9)$$

Different thermal diffusivity values approximately equal to the calculated values were assumed and used in the model to compare with the calculated values. The diffusivity at low depths was assumed constant and equal to that of the 35-40-cm depth layer. Table 1 shows the thermal diffusivity values as calculated from equations 8 and 9 used for determining the simulated subsoil temperature; bulk densities in this area as reported by Austin (1972) ranged from 1.1 to 1.5 with the mode at 1.2 g/cm^3. The value of c was arrived at from data in literature cited by Hanks and Jacobs (1971). They listed the value of c for most mineral soil to be from 0.18 to 0.22 cal·g^{-1}·°C^{-1}. Thus we chose 1.2 and 0.2 as bulk density and specific heat, respectively, as a good average to the complete profile. The thermal conductivity was calculated from the above values.

The change in heat content (heat flux when divided by the time interval) was calculated from:

$$\Delta HC = \sum_{i=1}^{n} (c\rho_{b_i} + \theta_i)\Delta T_i \cdot \Delta Z_i \qquad (10)$$

assuming the volumetric heat capacity of soil ($C_v = c\rho_{b_i} + \theta_i$) is known. Furthermore, a profile subsoil temperature of actual data and of simulated data from models was used. Both results were then compared.

Table 1. Thermal parameters used for determining the simulated subsoil temperature

Depth	Bulk density	Specific heat	Thermal diffusivity	Thermal conductivity
Z	ρ_b	c	λ	K
cm	g/cm^3	cal/g °C	cm^2/min	cal/cm min °C
0-5	1.2	0.2	0.13	0.032
5-10	1.2	0.2	0.23	0.056
10-15	1.2	0.2	0.31	0.073
15-20	1.2	0.2	0.35	0.085
20-25	1.2	0.2	0.36	0.086
25-30	1.2	0.2	0.37	0.088
30-35	1.2	0.2	0.39	0.093
35-40	1.2	0.2	0.40	0.095
40-45	1.2	0.2	0.40	0.095
45-50	1.2	0.2	0.40	0.095

Table 2. Calculated atmospheric radiation (incoming radiation from the atmosphere in ly/min) from 12 clear days during summer season, 1973

Hours	Jun 5	Jun 9	Jun 12	Jun 20	Jun 25	Jul 1	Jul 5	Jul 25	Aug 1	Aug 10	Aug 15	Aug 30
1	0.40	0.46	0.47	0.39	0.47	0.51	0.50	0.48	0.50	0.51	0.46	0.45
2	0.39	0.46	0.46	0.38	0.46	0.49	0.47	0.46	0.48	0.50	0.46	0.43
3.	0.38	0.46	0.46	0.37	0.45	0.47	0.45	0.44	0.46	0.50	0.45	0.43
4	0.38	0.46	0.45	0.36	0.45	0.45	0.44	0.44	0.45	0.50	0.45	0.42
5	0.38	0.47	0.46	0.37	0.45	0.44	0.45	0.44	0.45	0.50	0.45	0.43
6	0.40	0.49	0.47	0.39	0.47	0.45	0.47	0.46	0.47	0.51	0.47	0.45
7	0.42	0.50	0.48	0.41	0.49	0.46	0.49	0.47	0.49	0.52	0.49	0.47
8	0.44	0.52	0.49	0.42	0.50	0.47	0.51	0.49	0.51	0.53	0.50	0.49
9	0.44	0.53	0.51	0.44	0.52	0.47	0.53	0.50	0.52	0.55	0.51	0.49
10	0.44	0.54	0.52	0.46	0.53	0.48	0.55	0.52	0.54	0.56	0.52	0.50
11	0.44	0.55	0.52	0.48	0.54	0.48	0.56	0.53	0.55	0.57	0.53	0.51
12	0.46	0.56	0.52	0.49	0.55	0.48	0.57	0.54	0.56	0.57	0.55	0.53
13	0.47	0.61	0.52	0.50	0.55	0.49	0.57	0.54	0.56	0.57	0.56	0.55
14	0.48	0.61	0.52	0.51	0.55	0.49	0.57	0.55	0.57	0.58	0.57	0.55
15	0.48	0.55	0.52	0.51	0.56	0.48	0.59	0.55	0.56	0.58	0.56	0.54
16	0.48	0.55	0.51	0.51	0.56	0.48	0.59	0.55	0.56	0.57	0.56	0.52
17	0.48	0.55	0.51	0.51	0.55	0.48	0.59	0.55	0.55	0.56	0.55	0.50
18	0.48	0.55	0.50	0.50	0.55	0.49	0.57	0.55	0.53	0.55	0.55	0.50
19	0.46	0.54	0.50	0.49	0.54	0.49	0.55	0.52	0.52	0.54	0.55	0.49
20	0.46	0.53	0.49	0.48	0.53	0.48	0.53	0.50	0.50	0.52	0.54	0.48
21	0.45	0.52	0.48	0.48	0.52	0.48	0.52	0.49	0.49	0.51	0.53	0.48
22	0.44	0.51	0.48	0.47	0.51	0.47	0.51	0.49	0.48	0.51	0.51	0.47
23	0.44	0.50	0.48	0.47	0.50	0.46	0.50	0.48	0.47	0.50	0.50	0.47
24	0.43	0.49	0.47	0.46	0.49	0.45	0.50	0.48	0.47	0.50	0.48	0.46

Table 3. Observed global radiation (incoming solar and scattered radiation in ly/min) from 12 clear days during summer season, 1973

Hours	Jun 5	Jun 9	Jun 12	Jun 20	Jun 25	Jul 1	Jul 5	Jul 25	Aug 1	Aug 10	Aug 15	Aug 30
1	0.00	0.00	0.00	0.00	0.00	0.00	0.00	0.00	0.00	0.00	0.00	0.00
2	0.00	0.00	0.00	0.00	0.00	0.00	0.00	0.00	0.00	0.00	0.00	0.00
3	0.00	0.00	0.00	0.00	0.00	0.00	0.00	0.00	0.00	0.00	0.00	0.00
4	0.00	0.00	0.00	0.00	0.00	0.00	0.00	0.00	0.00	0.00	0.00	0.00
5	0.10	0.00	0.10	0.10	0.10	0.00	0.00	0.00	0.00	0.00	0.00	0.00
6	0.20	0.10	0.20	0.20	0.20	0.20	0.20	0.10	0.10	0.10	0.10	0.00
7	0.50	0.30	0.50	0.50	0.50	0.50	0.50	0.40	0.40	0.30	0.30	0.20
8	0.80	0.60	0.80	0.80	0.80	0.70	0.70	0.70	0.70	0.60	0.60	0.50
9	1.00	0.90	1.00	1.00	1.00	1.00	1.00	0.90	0.90	0.90	0.90	0.80
10	1.20	1.10	1.20	1.20	1.20	1.20	1.20	1.10	1.10	1.10	1.10	1.00
11	1.40	1.30	1.40	1.40	1.30	1.40	1.30	1.30	1.30	1.20	1.20	1.20
12	1.40	1.40	1.40	1.40	1.40	1.40	1.40	1.30	1.30	1.30	1.30	1.30
13	1.40	1.40	1.40	1.40	1.40	1.40	1.40	1.30	1.30	1.20	1.30	1.30
14	1.30	1.40	1.30	1.30	1.30	1.40	1.30	1.30	1.30	1.10	1.20	1.20
15	1.20	1.20	1.20	1.20	1.10	1.20	1.20	1.10	1.10	0.80	1.00	1.00
16	1.00	1.00	1.00	1.00	0.90	1.00	1.00	0.90	0.90	0.60	0.80	0.80
17	0.70	0.80	0.70	0.70	0.70	0.70	0.70	0.70	0.60	0.30	0.60	0.60
18	0.40	0.60	0.40	0.50	0.40	0.40	0.40	0.40	0.40	0.10	0.30	0.30
19	0.20	0.30	0.20	0.20	0.20	0.20	0.20	0.20	0.10	0.00	0.10	0.10
20	0.00	0.10	0.00	0.00	0.00	0.00	0.00	0.00	0.00	0.00	0.00	0.00
21	0.00	0.00	0.00	0.00	0.00	0.00	0.00	0.00	0.00	0.00	0.00	0.00
22	0.00	0.00	0.00	0.00	0.00	0.00	0.00	0.00	0.00	0.00	0.00	0.00
23	0.00	0.00	0.00	0.00	0.00	0.00	0.00	0.00	0.00	0.00	0.00	0.00
24	0.00	0.00	0.00	0.00	0.00	0.00	0.00	0.00	0.00	0.00	0.00	0.00

Table 2 shows the values of atmospheric radiation for several clear days as calculated by Angstrom's equation; these were used in the radiation model. Table 3 shows the hourly global radiation as observed on some clear days used, also, in the radiation model.

RESULTS AND DISCUSSION

The Radiation Balance -- Actual Data

The diurnal variation in radiation components on three clear days is shown in Figures 1, 2 and 3 where short-wave

solar and scattered radiation flux ($R_S + R_D$), net radiation flux (R_N) and albedo are all measured quantities in the field.

These three figures show that for each situation there was a noteworthy daily cycle. Net radiation was greater in the period of midday and morning than in the afternoon. These results agree with those of Monteith and Szeicz (1961), where net radiation was always less in the afternoon than in the morning. They attributed the difference to higher afternoon surface temperature along with an almost constant long-wave emission from the atmosphere.

Net radiation was usually slightly negative in the early morning and late afternoon (Figs. 1-3). This was because the emitted radiation from the surface is greater than the atmospheric radiation.

At midday and early afternoon, the heat loss by long-wave exchange ($R_A - R_E$) was (on July 9 and August 1) three times its nocturnal value, and twice the loss by short-wave reflection. A similar variation of the net long-wave term was reported by Monteith and Szeicz (1961).

The mean long-wave loss on clear days increased from 0.10 cal·cm^{-2}·min^{-1} before dawn to 0.29 cal·cm^{-2}·min^{-1} at midday when the maximum solar radiation was 1.39 cal·cm^{-2}·min^{-1} (on July 7 and July 9) and 1.34 cal·cm^{-2}·min^{-1} (on August 1).

Table 4 shows the diurnal variation in long-wave radiation (R_E and R_A) as calculated from observed data. The emitted radiation (R_E) varied from 0.46 cal·cm^{-2}·min^{-1} before sunrise to 1.03 cal·cm^{-2}·min^{-1} at midday (on July 7 and 9) and from 0.45 cal·cm^{-2}·min^{-1} to 0.92 cal·cm^{-2}·min^{-1} (on August 1).

On those days shown, the maximum atmospheric radiation (R_A) reached 0.75 cal·cm^{-2}·min^{-1} in the early afternoon and the minimum was 0.33 cal·cm^{-2}·min^{-1} before dawn when the emitted radiation was approximately 0.46 cal·cm^{-2}·min^{-1} and 1.02 cal·cm^{-2}·min^{-1}, respectively.

Compared with the calculated values presented in Table 2, these data derived from observations are slightly higher (0.12 ly/min at maximum). This inconsistency seems to be due to a change in calibration of the net radiometer in the long-wave range, particularly since the maximum of the R_A is also shifted somewhat to the earlier hours. Further observations are underway with this particular instrument.

Soil Temperature Profile -- Actual Data

The soil temperature as a function of time is presented in Figures 4, 5 and 6 (these data are in Tables 19, 20 and 21 in Apendix C). The maximum soil temperatures at the surface were found to occur at 1300,1400 and 1500 hr in each of the cited days. The maximum soil temperatures at 2-cm depth were reached at 1500, 1700 and 1600 hr, respectively; thus the time lag at 2-cm depth was 2½ hr on July 7 and 1 hr on July 9 and August 1.

Table 4. Emitted and atmospheric radiation (in ly/min) on July 7 and 9, calculated from observed data

Hours	July 7		July 9	
	R_E	R_A	R_E	R_A
1	0.500	0.366	0.469	0.372
2	0.483	0.362	0.465	0.371
3	0.481	0.362	0.461	0.369
4	0.466	0.339	0.460	0.372
5	0.458	0.329	0.478	0.383
6	0.466	0.329	0.549	0.453
7	0.527	0.407	0.659	0.529
8	0.627	0.447	0.778	0.608
9	0.730	0.510	0.853	0.653
10	0.820	0.570	0.925	0.692
11	0.925	0.660	1.005	0.720
12	1.008	0.728	1.025	0.713
13	1.002	0.732	1.008	0.715
14	0.976	0.746	0.939	0.687
15	0.942	0.732	0.868	0.658
16	0.858	0.678	0.775	0.615
17	0.789	0.639	0.672	0.552
18	0.683	0.563	0.609	0.519
19	0.615	0.485	0.544	0.468
20	0.562	0.442	0.525	0.411
21	0.534	0.414	0.516	0.413
22	0.518	0.408		

The amplitude of the diurnal wave at 2-cm depth was approximately 58% of that of the surface. At 10-cm depth it was 18% on July 7 and July 9 and 25% on August 1. At 25-cm depth the wave amplitude was 4% that of the surface on July 7 and July 9.

The maximum temperatures reached at the surface were 69.5, 71 and 62.5 C on July 7, July 9 and August 1, respectively. At 2-cm depth the maximum temperatures were 49.25, 51 and 44.75 C in the same order of days as above. At 10-cm depth the maximum temperatures were 31 and 32.25 C. Soil temperature at this depth approached air temperature between 2 and 8 m. At 2-cm depth the temperature of the soil was warmer than the air.

The data of Figures 4, 5 and 6 show that before dawn the variations of temperature were small (about 1 or 2 C) and the minimum temperature was reached before the sunrise. With the beginning of solar radiation, surface temperature began to rise very slowly at first and more rapidly after 0700 hr. The temperature gradually increased as time advanced until solar noon when the surface temperature began to decrease. Between 1300 and 1500 hr, soil surface temperature changed and thereafter dropped off rapidly in late afternoon.

After solar noon, the rate of temperature decrease was low (about 3 C/hr) and increased gradually to about 6 C/hr. A maximum of about 11 C/hr was reached between 1800 and 1900 hr. After this period, the rate was again low as temperatures began to decline more slowly.

It was also found that soil temperature at 25-cm depth had daily variations of 2-3 C. At 50-cm depth, almost no variations occurred. At 125-cm depth, the temperature was constant throughout the day.

Simulated Subsoil Temperature

To simulate the conditions of subsoil temperature, the apparent thermal diffusivity of soil was determined using the soil temperature records and plotting the diurnal cycle

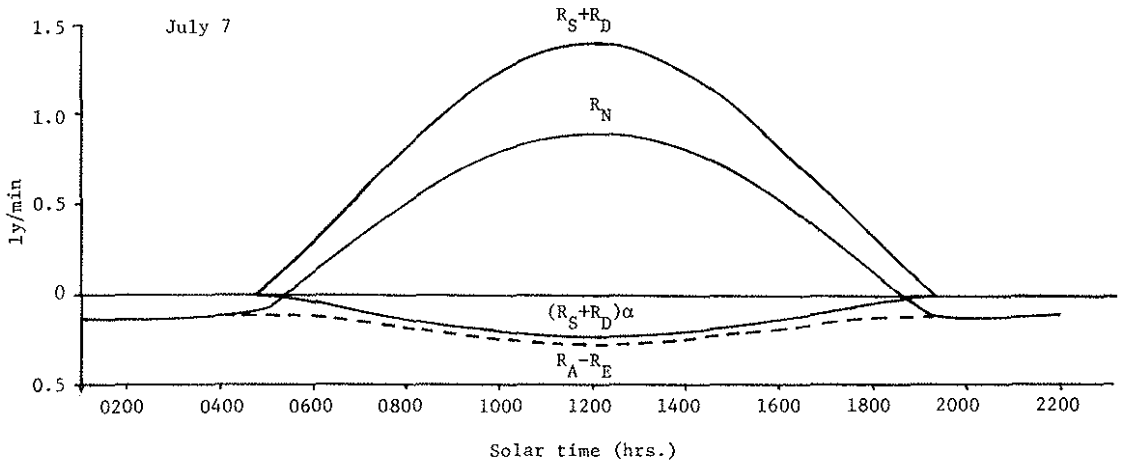

Figure 1. Observed variation of global radiation ($R_S + R_D$), net radiation (R_N), albedo $a(R_S + R_D)$ and net long-wave radiation ($R_A - R_E$) on July 7.

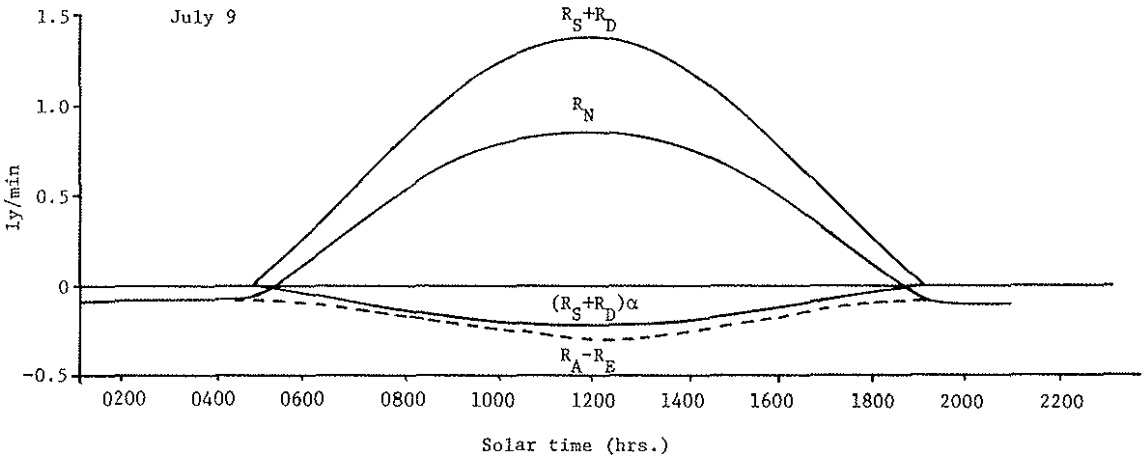

Figure 2. Observed variation of global radiation ($R_S + R_D$), net radiation (R_N), albedo $a(R_S + R_D)$ and net long-wave radiation ($R_A - R_E$) on July 9.

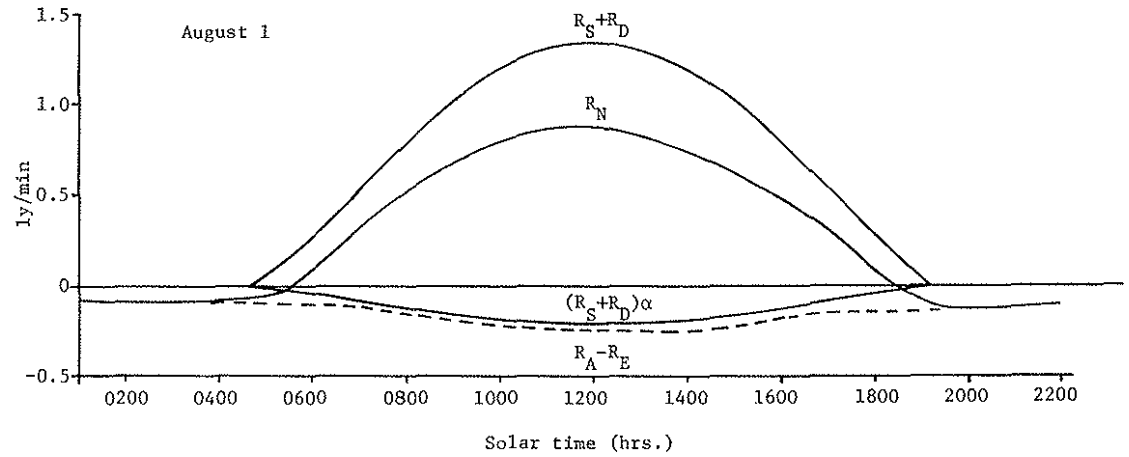

Figure 3. Observed variation of global radiation ($R_S + R_D$), net radiation (R_N), albedo $a(R_S + R_D)$ and net long-wave radiation ($R_A - R_E$) on August 1.

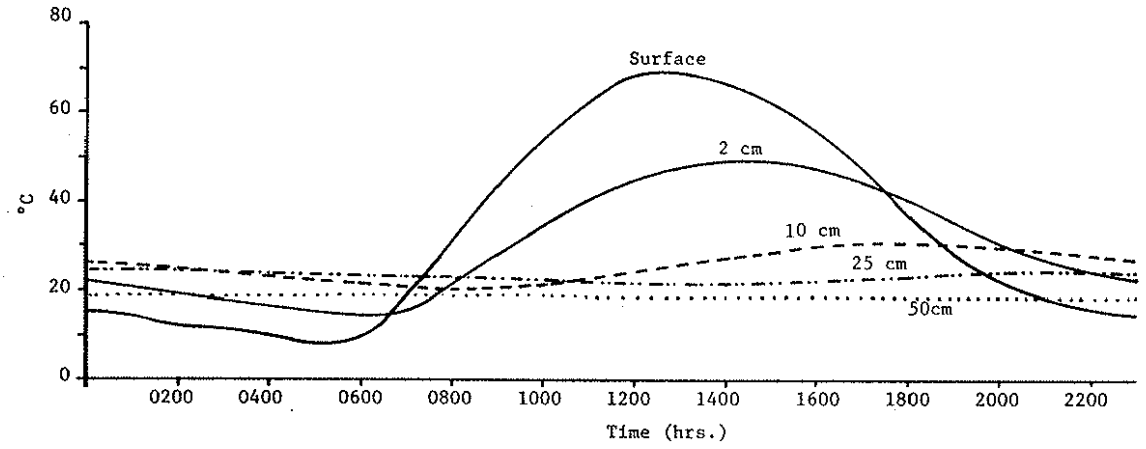

Figure 4. Observed soil temperature variation at 0-, 2-, 10-, 25- and 50-cm depths on July 7.

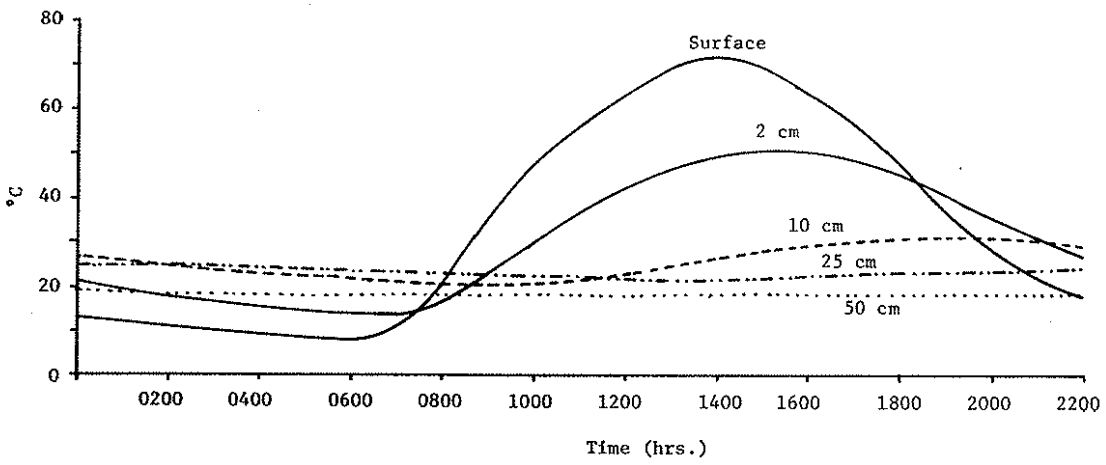

Figure 5. Observed soil temperature variation at 0-, 2-, 10-, 25- and 50-cm depths on July 9.

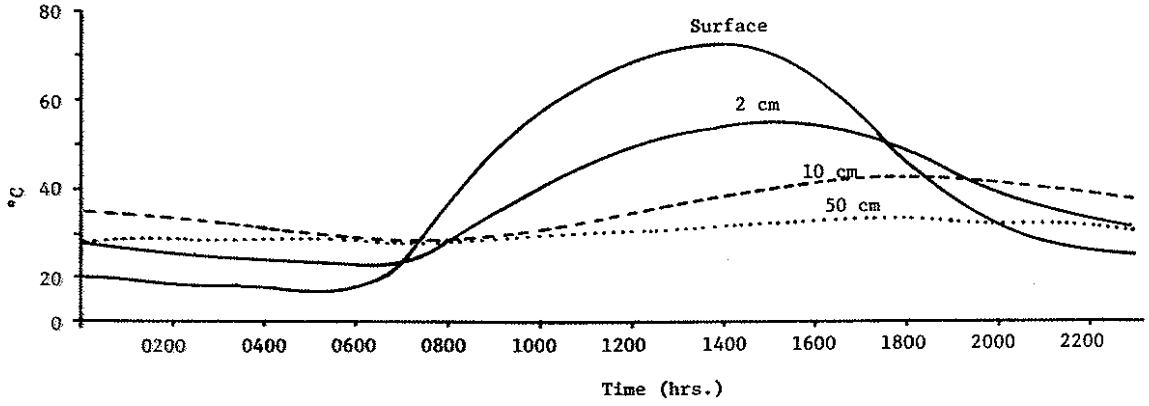

Figure 6. Observed soil temperature variation at 0-, 2-, 10- and 50-cm depths on August 1.

of each. Using the phase and amplitude relations, it was possible to get estimates of the variations of thermal diffusivity with depth. Diffusivity values obtained with the phase equation gave better results than those calculated with the amplitude equation. In the simulated situation, it was assumed that the diffusivity values calculated at various depths did not vary with time. Figures 7 and 8 show a comparison of two days (July 7 and July 9) between temperatures recorded in the field and temperatures simulated by the computer model. A close agreement was found between the measured values and computed values.

Since the soil temperatures recorded in the field were at 0-, 2-, 10-, 25-, 50- and 150-cm depths and the predicted temperatures were taken at layers of 5 cm each (5, 10, 15, 20, 25, 30, 35, 40, 45 and 50), it was only possible to compare exactly the temperatures at 10-, 25- and 50-cm depths. At 10-cm depth, soil temperature observed and predicted were in close agreement. This agreement was even better at 25 cm and particularly at 50 cm since nothing changed there.

Calculated Long-wave Radiation (R_E) -- *With Radiation Model*

Table 5 shows a comparison between several clear days of emitted radiation from the surface of soil as obtained by the radiation model. The calculated radiation varied from 0.44 ly/min (average value) at early hours in the morning to 1.66 ly/min (average value) at midday. In the morning there is no notable difference between radiation calculated from observed data in the field and that calculated with the radiation model, but at midday the difference was 0.63 ly/min. This is due to the suppression of all other heat change components except radiative transfer. The infinitesimal soil surface layer theoretically then heats up by far more than under natural conditions until radiative equilibrium is reached, thus resulting in these high values of R_E.

Calculated Surface Temperature -- With Radiation Model

Table 6 shows the hourly simulated temperature of the surface on several clear days as determined by the radiation

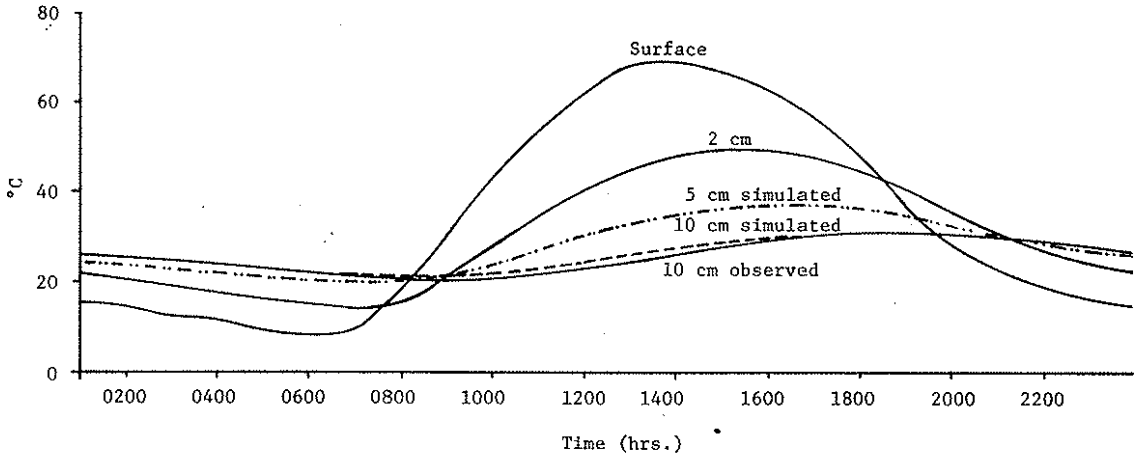

Figure 7. Observed and simulated soil temperature variation. The solid lines are the observed soil temperatures. The dots represent the computed soil temperatures on July 7.

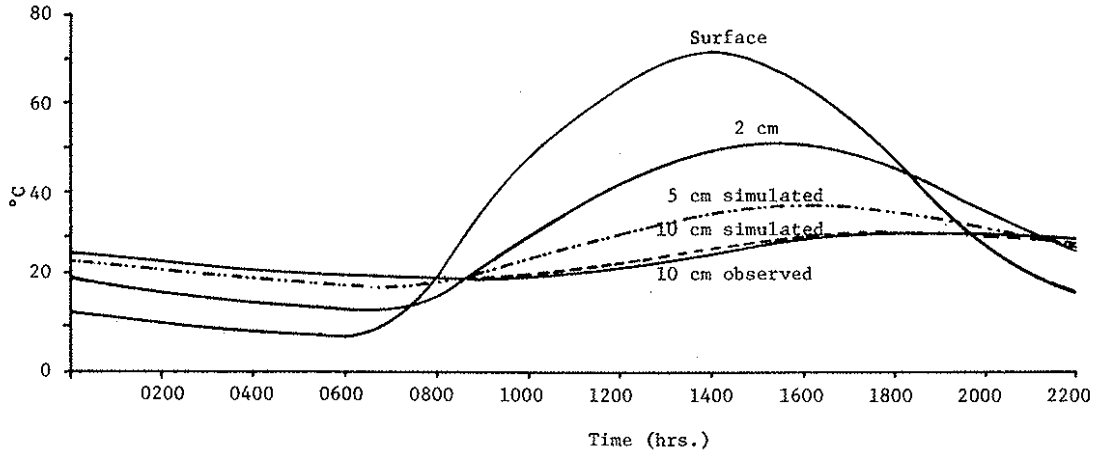

Figure 8. Observed and simulated soil temperature variation on July 9. The solid lines are the observed soil temperatures. The dots represent the computed soil temperatures.

Table 5. Calculated long-wave radiation, R_E, by radiation model (emitted radiation from the surface in ly/min) from 12 clear days during the summer season, 1973

Hours	Jun 5	Jun 9	Jun 12	Jun 20	Jun 25	Jul 1	Jul 5	Jul 25	Aug 1	Aug 1	Aug 15	Aug 30
1	0.40	0.46	0.47	0.39	0.47	0.51	0.50	0.48	0.50	0.51	0.46	.0.45
2	0.39	0.46	0.46	0.48	0.46	0.49	0.47	0.46	0.48	0.50	0.46	.0.43
3	0.38	0.46	0.46	0.37	0.45	0.47	0.45	0.44	0.46	0.50	0.45	0.43
4	0.42	0.47	0.50	0.41	0.49	0.48	0.47	0.44	0.46	0.50	0.45	0.42
5	0.58	0.53	0.65	0.57	0.64	0.61	0.61	0.56	0.56	0.58	0.53	0.47
6	0.83	0.74	0.88	0.82	0.88	0.84	0.86	0.80	0.80	0.79	0.75	0.64
7	1.08	1.02	1.12	1.06	1.12	1.08	1.11	1.05	1.05	1.03	1.00	0.90
8	1.30	1.26	1.34	1.28	1.34	1.30	1.34	1.20	1.27	1.25	1.24	1.14
9	1.47	1.45	1.52	1.47	1.51	1.50	1.53	1.46	1.46	1.45	1.43	1.34
10	1.59	1.60	1.65	1.60	1.64	1.63	1.66	1.59	1.59	1.58	1.56	1.48
11	1.64	1.71	1.71	1.67	1.70	1.68	1.72	1.66	1.66	1.65	1.63	1.56
12	1.65	1.74	1.71	1.69	1.70	1.68	1.72	1.66	1.67	1.58	1.63	1.60
13	1.59	1.70	1.64	1.63	1.64	1.62	1.67	1.60	1.62	1.46	1.56	1.55
14	1.46	1.60	1.51	1.50	1.52	1.49	1.56	1.48	1.59	1.28	1.44	1.42
15	1.28	1.43	1.33	1.33	1.34	1.30	1.39	1.31	1.32	1.06	1.26	1.22
16	1.07	1.23	1.11	1.12	1.14	1.09	1.19	1.10	1.09	0.83	1.04	0.98
17	0.83	1.02	0.88	0.89	0.92	0.86	0.95	0.87	0.84	0.63	0.80	0.74
18	0.61	0.79	0.65	0.66	0.70	0.64	0.72	0.65	0.62	0.55	0.61	0.55
19	0.48	0.60	0.52	0.52	0.56	0.51	0.57	0.64	0.56	0.54	0.55	0.49
20	0.46	0.53	0.49	0.48	0.53	0.48	0.53	0.50	0.50	0.52	0.54	0.48
21	0.45	0.52	0.48	0.48	0.52	0.48	0.52	0.49	0.49	0.51	0.53	0.48
22	0.44	0.51	0.48	0.47	0.51	0.47	0.51	0.49	0.48	0.51	0.51	0.47
23	0.44	0.50	0.48	0.47	0.50	0.46	0.50	0.48	0.47	0.50	0.50	0.47
24	0.43	0.49	0.47	0.46	0.49	0.45	0.50	0.48	0.47	0.50	0.48	0.46

Table 6. Calculated surface temperature (in °C) obtained from radiation model for 12 clear days in summer season, 1973

Hours	Jun5	Jun 9	Jun 12	Jun 20	Jun 25	Jul 1	Jul 5	Jul 25	Aug 1	Aug 1	Aug 15	Aug 30
1	-0.61	10.67	8.13	-2.38	9.98	16.52	14.67	11.00	14.67	16.02	9.21	6.70
2	-3.46	8.92	7.92	-5.40	7.91	12.63	10.28	8.00	10.79	14.80	7.74	4.44
3	-5.08	7.85	8.20	-7.16	6.74	9.48	7.43	5.00	8.22	14.10	6.78	3.13
4	1.70	13.76	10.25	-0.29	12.81	11.62	10.60	6.00	8.06	13.93	6.57	2.87
5	24.92	33.77	18.71	23.87	33.23	28.65	29.54	22.00	22.71	25.14	18.93	9.61
6	53.38	58.50	44.54	52.18	58.46	54.53	56.51	50.00	50.30	48.74	44.92	33.01
7	75.22	78.94	71.32	74.22	78.90	75.66	78.03	72.00	72.74	70.98	69.09	59.71
8	91.84	94.86	89.04	90.67	94.51	92.27	94.66	90.00	90.16	88.48	87.68	80.21
9	103.53	106.39	102.27	103.34	106.04	105.48	106.96	102.00	102.59	102.02	100.67	94.53
10	110.66	114.34	111.62	111.72	113.74	113.20	114.80	111.00	110.86	110.47	109.04	104.08
11	113.88	118.11	117.59	115.84	117.52	116.35	118.47	114.00	115.23	114.30	112.95	109.09
12	114.63	117.69	119.52	116.49	117.39	116.22	118.32	115.00	115.85	110.25	113.15	111.16
13	111.12	113.78	117.35	112.94	113.74	112.60	115.61	111.00	112.53	102.51	109.25	108.25
14	103.00	105.78	111.27	105.39	106.26	104.36	108.80	104.00	105.48	90.33	101.42	100.33
15	90.75	93.97	100.85	93.76	94.90	92.18	98.47	92.00	93.71	74.06	89.16	85.92
16	74.49	78.16	87.14	78.47	80.23	76.05	83.92	77.00	76.42	52.96	72.30	67.24
17	53.67	57.91	70.34	58.85	61.29	55.79	64.79	57.00	54.53	32.07	50.38	46.51
18	28.59	34.46	49.27	34.57	39.37	32.89	41.50	33.00	30.77	21.27	29.54	21.59
19	11.52	17.57	28.29	16.89	23.12	16.01	24.08	33.00	22.40	19.44	20.74	12.95
20	7.92	13.07	18.00	12.09	18.54	11.92	18.46	14.00	14.74	17.80	19.66	11.81
21	6.98	12.19	16.85	11.00	17.23	11.07	16.65	13.00	13.05	16.44	18.23	10.82
22	6.11	11.41	15.41	10.06	15.83	9.86	15.39	12.00	11.58	15.41	16.44	10.06
23	5.25	10.77	14.03	9.30	14.33	8.29	14.72	11.00	10.33	14.74	14.80	9.43
24	4.34	10.28	12.34	8.69	12.75	6.36	14.66	11.00	9.27	14.44	11.81	8.71

model. The high temperature obtained at the surface of the soil represents the temperature of the soil if no dissipation of heat occurs horizontally and vertically in the layers adjacent to the thin layer of the surface.

A comparison of the minimum temperatures of the surface as observed in the field on July 7 and 9 with those calculated by the radiation model on July 5, shows good agreement. However, the maximum calculated values obtained at midday and early in the afternoon are approximately 48 C higher than the measured values.

Simulated Subsoil Temperature Using Calculated Surface Temperature Obtained with Radiation Model

A simulated profile of soil temperature was determined with the radiation model. From Tables 7, 8 and 9 it can be seen that high differences of temperature result between these calculated values and the actual temperatures that occur in the top layers. These differences gradually decrease with depth and at 50-cm depth no difference is found. Thus, the heat formed at the surface does not reach that depth (50 cm) and probably did not even reach levels some centimeters above this depth.

At 25-cm depth, the differences in the maximum temperature between observed and calculated-for-simulation were 5.5 C (on July 7), 5.7 C (on July 9) and 3.5 C (on August 1) and occurred in the evening. The differences for minimum values were 1.0 C (on July 7), 1.7 C (on July 9) and 0.7 C (on August 1) and occurred in the morning.

At 10 cm, the differences of maximum values were 13.2 C (on July 7), 13.5 C (on July 9) and 12.0 C (on August 1). The differences of minimum values were 2.7 C, 3.8 C and 3.5 C, respectively.

At the surface, the differences of the maximum temperature were 49.0 C (on July 7), 51.3 C (on July 9) and 53.3 C (on August 1). The minimum differences were 0.9 C, 1.1 C and 0.9 C, respectively.

These values indicate the possible losses of heat by conduction in the several layers of the soil. The higher loss is found at the top of the soil.

Heat Flow in the Soil

The change in heat content in the soil was calculated by equation 10 using data of subsoil profile temperature observed in the field and assuming the volumentric heat capacity of soil (C_V) is known.

If we consider the volumetric heat capacity of soil to be constant (C_V) all over the profile, the variation of heat flux through the several layers below the soil surface between 5 a.m. and 2 p.m. on typical clear days is as shown in Tables 10, 11 and 12. The flow in the first layer (0- to 2-cm depth) represents 37% (on July 7), 33% (on July 9) and 30% (on August 1) of the overall profile. In the second layer (2- to 10-cm depth) the heat flow was 60% (on July 7) and 59% (on July 9 and August 1). Thus, the heat flow was concentrated in these first two layers.

Table 7. Hourly subsoil profile temperature determined from hourly surface temperature (from radiation model) on July 7

Hours	surface	5	10	15	20	25	30	35	40	45	50 cm
1	14.7	24.6	25.8	25.8	25.2	24.3	23.3	22.2	21.1	20.1	19.0
2	10.3	23.2	25.1	25.3	24.9	24.1	23.2	22.2	21.1	20.1	19.0
3	7.4	21.9	24.3	24.8	24.6	23.9	23.1	22.1	21.1	20.1	19.0
4	10.6	21.4	23.6	24.3	24.2	23.7	22.9	22.0	21.1	20.0	19.0
5	29.5	23.1	23.4	23.9	23.9	23.5	22.8	21.9	21.0	20.0	19.0
6	56.1	27.1	24.1	23.7	23.6	23.2	22.6	21.8	20.9	20.0	19.0
7	78.0	32.2	25.7	24.1	23.5	23.0	22.4	21.7	20.9	20.0	19.0
8	94.6	37.5	28.0	24.9	23.7	23.0	22.3	21.6	20.8	19.9	19.0
9	106.9	42.5	30.7	26.1	24.2	23.1	22.3	21.5	20.7	19.9	19.0
10	114.8	47.0	33.4	27.6	25.0	23.4	22.4	21.5	20.7	19.9	19.0
11	118.5	50.8	36.1	29.2	25.9	23.9	22.6	21.6	20.7	19.8	19.0
12	118.3	53.7	38.6	30.9	27.0	24.5	22.9	21.7	20.7	19.9	19.0
13	115.6	55.7	40.7	32.5	28.1	25.2	23.3	21.9	20.8	19.9	19.0
14	108.8	56.7	42.4	34.0	29.3	26.0	23.8	22.2	21.0	20.0	19.0
15	98.5	56.5	43.6	35.3	30.4	26.9	24.3	22.5	21.2	20.0	19.0
16	83.9	55.1	44.2	36.3	31.4	27.7	24.9	22.9	21.4	20.1	19.0
17	64.8	52.2	44.0	37.0	32.2	28.4	25.5	23.3	21.6	20.3	19.0
18	41.5	47.8	43.0	37.2	32.8	29.1	26.0	23.7	21.9	20.4	19.0
19	24.1	43.0	41.3	37.0	33.2	29.6	26.5	24.1	22.2	20.5	19.0
20	18.5	39.2	39.4	36.4	33.2	29.9	26.9	24.5	22.4	20.6	19.0
21	16.7	36.3	37.5	35.5	32.9	30.0	27.2	24.7	22.6	20.8	19.0
22	15.4	34.0	35.8	34.6	32.5	30.0	27.4	25.0	22.8	20.9	19.0
23	14.7	32.2	34.3	33.6	32.0	29.8	27.4	25.1	23.0	20.9	19.0
24	14.6	30.7	32.9	32.7	31.5	29.6	27.3	25.2	23.0	21.0	19.0

Table 8. Hourly subsoil profile temperature determined from hourly surface temperature (from radiation model) on July 9

Hours	surface	5 cm	10	15	20	25	30	35	40	45	50 cm
1	16.7	25.6	26.8	26.6	25.5	24.5	23.5	22.5	21.5	20.4	19.3
2	10.3	24.1	25.9	25.9	25.1	24.5	23.5	22.4	21.4	20.4	19.3
3	7.4	22.7	25.0	25.4	25.0	24.3	23.4	22.4	21.4	20.4	19.3
4	10.6	22.0	24.3	24.9	24.7	24.1	23.3	22.3	21.4	20.3	19.3
5	29.5	23.6	24.0	24.4	24.3	23.9	23.1	22.3	21.3	20.3	19.3
6	56.1	27.6	24.6	24.3	24.1	23.6	23.0	22.2	21.3	20.3	19.3
7	78.0	32.7	26.3	24.6	24.0	23.5	22.8	22.0	21.2	20.3	19.3
8	94.6	37.9	28.5	25.4	24.2	23.4	22.7	22.0	21.1	20.2	19.3
9	106.9	42.9	31.1	26.6	24.7	23.6	22.7	21.9	21.1	20.2	19.3
10	114.8	47.4	33.9	28.0	25.4	23.8	22.8	21.9	21.0	20.2	19.3
11	118.5	51.2	36.5	29.6	26.3	24.3	23.0	21.9	21.0	20.2	19.3
12	118.3	54.0	39.0	31.3	27.4	24.9	23.3	22.1	21.1	20.2	19.3
13	115.6	56.0	41.1	32.9	28.6	25.6	23.7	22.3	21.2	20.2	19.3
14	108.8	57.0	42.8	34.4	29.7	26.4	24.1	22.5	21.3	20.3	19.3
15	98.5	56.8	44.0	35.7	30.8	27.3	24.7	22.9	21.5	20.4	19.3
16	83.9	55.4	44.5	36.7	31.8	28.1	25.3	23.3	21.7	20.5	19.3
17	64.8	52.5	44.3	37.4	32.6	28.8	25.8	23.7	22.0	20.6	19.3
18	41.5	48.1	43.3	37.6	33.2	29.4	26.4	24.1	22.2	20.7	19.3
19	24.1	43.3	41.7	37.4	33.5	29.9	26.9	24.5	22.5	20.8	19.3
20	18.5	39.5	39.7	36.7	33.5	30.2	27.3	24.8	22.8	21.0	19.3
21	16.7	36.6	37.8	35.9	33.3	30.4	27.5	25.1	23.0	21.1	19.3
22	15.4	34.2	36.1	34.9	32.9	30.3	27.7	25.3	23.2	21.2	19.3
23	14.7	32.4	34.5	33.9	32.4	30.2	27.7	25.4	23.3	21.3	19.3
24	14.6	30.9	33.2	33.0	31.8	29.9	27.7	25.5	23.4	21.3	19.3

Table 9. Hourly subsoil profile temperature determined from hourly surface temperature (from radiation model) on August 1

Hours	surface	5 cm	10	15	20	25	30	35	40	45	50 cm
1	14.7	21.7	23.9	24.4	24.0	23.3	22.4	21.5	20.5	19.6	18.7
2	10.8	21.1	23.2	23.8	23.7	23.1	22.3	21.4	20.5	19.6	18.7
3	8.2	20.3	22.6	23.3	23.3	22.9	22.2	21.4	20.5	19.6	18.7
4	8.1	19.6	22.0	22.9	23.0	22.6	22.0	21.3	20.5	19.6	18.7
5	22.7	20.8	21.7	22.5	22.6	22.4	21.9	21.2	20.4	19.6	18.7
6	50.3	24.6	22.3	22.3	22.3	22.1	21.7	21.1	20.3	19.5	18.7
7	72.7	29.6	23.8	22.6	22.3	22.0	21.5	20.9	20.3	19.5	18.7
8	90.2	34.9	26.1	23.3	22.4	21.9	21.4	20.8	20.2	19.5	18.7
9	102.6	40.0	28.7	24.5	22.9	22.0	21.4	20.8	20.1	19.4	18.7
10	110.9	44.6	31.4	25.9	23.6	22.3	21.4	20.7	20.1	19.4	18.7
11	115.2	48.4	34.2	27.6	24.5	22.8	21.6	20.8	20.1	19.4	18.7
12	115.8	51.5	36.7	29.2	25.6	23.4	21.9	20.9	20.1	19.4	18.7
13	112.5	53.5	38.8	30.9	26.7	24.1	22.3	21.1	20.2	19.4	18.7
14	105.5	54.5	40.5	32.4	27.9	24.9	22.8	21.4	20.4	19.5	18.7
15	93.7	54.1	41.7	33.7	29.0	25.7	23.3	21.7	20.5	19.6	18.7
16	76.4	52.3	42.2	34.7	30.0	26.5	23.9	22.1	20.8	19.7	18.7
17	54.5	48.8	41.8	35.3	30.8	27.2	24.5	22.5	21.0	19.8	18.7
18	30.7	43.9	40.6	35.4	31.4	27.8	25.0	22.9	21.3	19.9	18.7
19	22.4	39.9	38.8	35.1	31.6	28.3	25.5	23.3	21.5	20.0	18.7
20	14.7	36.2	36.9	34.4	31.6	28.6	25.9	23.6	21.8	20.2	18.7
21	13.1	33.5	35.1	33.6	31.3	28.7	26.1	23.9	22.0	20.3	18.7
22	11.6	31.2	33.4	32.6	30.9	28.6	26.2	24.1	22.2	20.4	18.7
23	10.3	29.3	31.9	31.7	30.4	28.4	26.3	24.2	22.3	20.5	18.7
24	9.3	27.7	30.6	30.8	29.8	28.2	26.2	24.2	22.4	20.5	18.7

Table 10. Heat flow calculated of observed values of soil temperature in the field on July 7

DEPTH (cm)	T (°C) at 5 A.M.	T (°C) at 2 P.M.	ΔT °C	ΔZ cm	ΔT.ΔZ °C.cm	ΔHC cal.cm.$^{-2}$	%	Cv	ΔHC cal.cm.$^{-2}$	%
0 - 2	11.63	58.00	46.37	2	92.74	92.74 Cv	36.8	0.39	36.16	35.3
2 - 10	18.75	38.50	19.75	8	158.00	158.00 Cv	62.7	0.43	67.94	66.4
10 - 25	23.13	24.88	1.75	15	26.25	26.25 Cv	10.4	0.49	12.86	12.6
25 - 50	21.50	20.50	-1.00	25	-25.00	-25.00 Cv	-9.9	0.59	-14.75	-14.4
TOTAL						251.99 Cv			102.21	

Table 11. Heat flow calculated of observed values of soil temperature in the field on July 9

DEPTH (cm)	T (°C) at 5 A.M.	T (°C) at 2 P.M.	ΔT °C	ΔZ cm	ΔT.ΔZ °C.cm	ΔHC cal.cm.$^{-2}$	%	Cv	ΔHC cal.cm.$^{-2}$	%
0 - 2	11.25	60.25	49.00	2	98.00	98.00 Cv	33.0	0.39	38.22	30.9
2 - 10	17.75	39.62	21.87	8	174.96	174.96 Cv	58.9	0.43	75.23	60.8
10 - 25	22.50	25.13	2.63	15	39.45	39.45 Cv	13.3	0.49	19.33	15.6
25 - 50	21.25	20.63	-0.62	25	-15.50	-15.50 Cv	-5.2	0.59	-9.14	-7.4
TOTAL						296.91 Cv			123.64	

Table 12. Heat flow calculated of observed values of soil temperature in the field on August 1

DEPTH (cm)	T (°C) at 5 A.M.	T (°C) at 2 P.M.	ΔT °C	ΔZ cm	ΔT.ΔZ °C.cm	ΔHC cal.cm.$^{-2}$	%	Cv	ΔHC cal.cm.$^{-2}$	%
0 - 2	10.38	52.50	42.12	2	84.24	84.24 Cv	29.8	0.39	32.85	28.3
2 - 10	16.25	37.25	21.00	8	168.00	168.00 Cv	59.4	0.43	72.24	62.2
10 - 25	21.13	25.88	4.75	15	71.25	71.25 Cv	25.1	0.49	34.91	30.1
25 - 50	20.63	22.25	-1.62	25	-40.50	-40.50 Cv	-14.3	0.59	-23.89	-20.6
TOTAL						282.99 CV			116.11	

With varying volumetric heat capacity (Tables 10, 11 and 12) we found the following percentages: the first layer, 35% (on July 7), 31% (on July 9) and 28% (on August 1). In the second layer (2- to 10-cm depth) 66% (on July 7), 75% (on July 9) and 72% (on August 1).

The daily net heat gain was relatively small indicating that most of the ΔHC gained during the day was lost during the night.

Calculated Heat Flow in the Soil Using Data of Simulated Profile of Subsoil Temperature

Data of simulated subsoil profile temperature were used to calculate heat flow with formula 10. The maximum flow of heat was concentrated in the first 10-cm depth. Tables 13, 14 and 15 show the following percentages: July 7, 97%; July 9, 93.4%; 92% on August 1. These high percentages were calculated for the 0- to 10-cm depth, observing C_v to be constant throughout the profile.

With estimated values of the volumetric heat capacity, we found 99% on July 7, 94.5% on July 9 and 93% on August 1 for the first two layers. These values indicate a good agreement if compared with the calculated values using the observed data of temperature in the field. Furthermore, very little downward flux occurs in layers below 10-cm depth.

Tables 16, 17 and 18 show the calculated heat flow using the temperature profiles of Tables 7, 8 and 9, respectively. In the two first layers (0- to 10-cm depth) we found the following percentages: 74%, July 7; 74%, July 9; 75%, August 1, for constant C_v throughout the profile. For varying C_v, percentages of 70 on July 7, 69 on July 9 and 71 on August 1 were found.

CONCLUSIONS

For equal short-wave radiation intensities, the net radiation was always less in the afternoon than in the morning because of higher afternoon surface temperature. The diurnal changes were much greater in the outgoing than in the incoming component of long-wave radiation.

At midday and early afternoon, the heat loss by long-wave exchange was approximately three times its

Table 13. Heat flow calculated from simulated values of subsoil profile temperature on July 7

DEPTH (cm)	T (°C) at 5 A.M.	T (°C) at 2 P.M.	ΔT °C	ΔZ cm	ΔT.ΔZ °C.cm	ΔHC cal.cm^{-2}	%	Cv	ΔHC cal.cm^{-2}	%
0 - 5	14.25	51.50	37.25	5	186.25	186.25 Cv	74.6	0.39	72.64	75.9
5 -10	21.50	32.70	11.20	5	56.00	56.00 Cv	22.4	0.40	22.40	23.4
10-15	23.10	27.25	4.15	5	20.75	20.75 Cv	8.3	0.43	8.92	9.3
15-20	23.55	24.50	0.95	5	4.75	4.75 Cv	1.9	0.54	2.57	2.6
20-25	23.40	23.00	-0.40	5	-2.00	-2.00 Cv	-0.8	0.54	-1.08	-1.1
25-30	22.90	22.00	-0.90	5	-4.50	-4.50 Cv	-1.8	0.54	-2.43	-2.53
30-35	22.20	21.25	-0.95	5	-4.75	-4.75 Cv	-1.9	0.67	-3.18	-3.32
35-40	21.35	20.60	-0.75	5	-3.75	-3.75 Cv	-1.5	0.67	-2.51	-2.6
40-45	20.45	20.00	-0.45	5	-2.25	-2.25 Cv	-0.9	0.54	-1.22	-1.3
45-50	19.50	19.35	-0.15	5	-0.75	-0.75 Cv	-0.3	0.54	-0.40	-0.4
TOTAL						249.75 Cv			95.71	

Table 14. Heat flow calculated from simulated values of subsoil profile temperature on July 9

DEPTH (cm)	T (°C) at 5 A.M.	T (°C) at 2 P.M.	T °C	Z cm	T. Z °C. cm	HC cal.cm^{-2}	%	Cv	HC cal.cm^{-2}	%
0 - 5	14.10	53.25	39.15	5	195.75	195.75 Cv	71.1	0.39	76.34	71.5
5 -10	20.90	33.20	12.30	5	61.50	61.50 Cv	22.3	0.40	24.60	23.0
10-15	22.60	27.50	4.90	5	24.50	24.50 Cv	8.9	0.43	10.53	9.9
15-20	23.20	24.65	1.45	5	7.25	7.25 Cv	2.6	0.54	3.91	3.7
20-25	23.20	23.10	-0.10	5	-0.50	-0.50 Cv	-0.2	-.54	-0.27	-0.3
25-30	22.55	22.10	-0.45	5	-2.25	-2.25 Cv	-0.8	0.54	-1.21	-1.1
30-35	22.25	21.35	-0.90	5	-4.50	-4.50 Cv	-1.6	0.67	-3.01	-2.8
35-40	21.50	20.75	-0.75	5	-3.75	-3.75 Cv	-1.3	0.67	-2.51	-2.3
40-45	20.65	20.20	-0.45	5	-2.25	-2.25 Cv	-0.8	0.54	-1.21	-1.1
45-50	19.75	19.60	-0.15	5	-0.75	-0.75 Cv	-0.2	0.54	-0.40	-0.4
TOTAL						275.50 Cv			106.77	

Table 15. Heat flow calculated from simulated values of subsoil profile temperature on August 1

DEPTH (cm)	T (°C) at 5 A.M.	T (°C) at 2 P.M.	ΔT °C	ΔZ cm	ΔT.ΔZ °C.cm	ΔHC cal.cm^{-2}	%	Cv	ΔHC cal.cm^{-2}	%
0 - 5	13.05	47.10	34.05	5	170.25	170.25 Cv	69.0	0.39	66.39	69.1
5 -10	19.30	30.70	11.40	5	57.00	57.00 Cv	23.1	0.40	22.80	23.7
10-15	21.00	25.85	4.85	5	24.25	24.25 Cv	9.8	0.43	10.42	10.8
15-20	21.70	23.35	1.65	5	8.25	8.25 Cv	3.3	0.54	4.45	4.6
20-25	21.85	21.95	0.10	5	0.50	0.50 Cv	0.2	0.54	0.27	0.3
25-30	21.65	21.05	-0.60	5	-3.00	-3.00 Cv	-1.2	0.54	-1.62	-1.7
30-35	21.20	20.40	-0.80	5	-4.00	-4.00 Cv	-1.6	0.67	-2.68	-2.8
35-40	20.60	19.90	-0.70	5	-3.50	-3.50 Cv	-1.4	0.67	-2.34	-2.4
40-45	19.90	19.45	-0.45	5	-2.25	-2.25 Cv	-0.9	0.54	-1.21	-1.3
45-50	19.10	18.95	-0.15	5	-0.75	-0.75 Cv	-0.3	0.54	-0.40	-0.4
TOTAL						246.75 Cv			96.08	

Table 16. Heat flow calculated from data of profile temperature from Table 7

DEPTH (cm)	T (°C) at 5 A.M.	T (°C) at 2 P.M.	ΔT °C	ΔZ cm	ΔT.ΔZ °C.cm	ΔHC cal.cm^{-2}	%	Cv	ΔHC cal.cm^{-2}	%
0 - 5	26.30	82.75	56.54	5	282.25	282.25 Cv	50.6	0.39	110.07	47.3
5 -10	23.25	49.55	26.30	5	131.50	131.50 Cv	23.6	0.40	52.60	22.6
10-15	23.65	38.20	14.55	5	72.75	72.75 Cv	13.0	0.43	31.28	13.4
15-20	23.90	31.65	7.75	5	38.75	38.75 Cv	6.9	0.54	20.92	9.0
20-25	23.70	27.65	3.95	5	19.75	19.75 Cv	3.5	0.54	10.66	4.6
25-30	23.15	24.90	1.75	5	8.75	8.75 Cv	1.6	0.54	4.72	2.0
30-35	22.35	23.00	0.65	5	3.25	3.25 Cv	0.6	0.67	2.17	0.9
35-40	21.45	21.60	0.15	5	0.75	0.75 Cv	0.1	0.67	0.50	0.2
40-45	20.50	20.50	0.00	5	0.00	0.00 Cv	0.0	0.54	0.00	0.0
45-50	19.50	19.50	0.00	5	0.00	0.00 Cv	0.0	0.54	0.00	0.0
TOTAL						557.75 Cv			232.92	

Table 17. Heat flow calculated from data of profile temperature from Table 8

DEPTH (cm)	T (°C) at 5 A.M.	T (°C) at 2 P.M.	ΔT °C	ΔZ cm	ΔT.ΔZ °C.cm	ΔHC cal.cm^{-2}	%	Cv	ΔHC cal.cm^{-2}	%
0 - 5	26.55	82.90	56.35	5	281.75	281.75 Cv	50.8	0.39	109.88	47.5
5 -10	23.80	49.90	26.10	5	130.50	130.50 Cv	23.5	0.40	52.20	22.5
10-15	24.20	38.60	14.40	5	72.00	72.00 Cv	13.0	0.43	30.96	13.4
15-20	24.35	32.05	7.70	5	38.50	38.50 Cv	6.9	0.54	20.79	9.0
20-25	24.10	28.05	3.95	5	19.75	19.75 Cv	3.6	0.54	10.66	4.6
25-30	23.50	25.25	1.75	5	8.75	8.75 Cv	1.6	0.54	4.72	2.0
30-35	22.70	23.30	0.60	5	3.00	3.00 Cv	0.5	0.67	2.01	0.9
35-40	21.80	21.90	0.10	5	0.50	0.50 Cv	0.1	0.67	0.33	0.1
40-45	20.80	20.80	0.00	5	0.00	0.00 Cv	0.0	0.54	0.00	0.0
45-50	19.80	19.80	0.00	5	0.00	0.00 Cv	0.0	0.54	0.00	0.0
TOTAL						554.75 Cv			231.55	

Table 18. Heat flow calculated from data of subsoil profile temperature from Table 9

DEPTH (cm)	T (°C) at 5 A.M.	T (°C) at 2 P.M.	ΔT °C	ΔZ cm	ΔT.ΔZ °C.cm	ΔHC cal.cm^{-2}	%	Cv	ΔHC cal.cm^{-2}	%
0 - 5	21.75	80.00	58.25	5	291.25	291.25 Cv	51.73	0.39	113.58	48.43
5 -10	21.25	47.50	26.25	5	131.25	131.25 Cv	23.31	0.40	52.50	22.38
10-15	22.10	36.45	14.35	5	71.75	71.75 Cv	12.74	0.43	30.85	13.15
15-20	22.55	30.15	7.60	5	38.00	38.00 Cv	6.75	0.54	20.52	8.75
20-25	22.50	26.40	3.90	5	19.50	19.50 Cv	3.46	0.54	10.53	4.49
25-30	22.15	23.85	1.70	5	8.50	8.50 Cv	1.51	0.54	4.59	1.95
30-35	21.55	22.10	0.55	5	2.75	2.75 Cv	0.49	0.67	1.84	0.78
35-40	20.80	20.90	0.10	5	0.50	0.50 Cv	0.09	0.67	0.34	0.14
40-45	20.00	19.95	-0.95	5	-0.25	-0.25 Cv	-0.04	0.54	-0.13	-0.05
45-50	19.15	19.10	-0.05	5	-0.25	-0.25 Cv	-0.04	0.54	-0.13	-0.05
TOTAL						563.00 Cv			234.49	

nocturnal value. At midday the atmospheric radiation calculated from observed data was about 70% of the emitted long-wave radiation from the surface. The value of the long-wave radiation (R_E) at midday, derived from the radiation model (average value of 12 days), was 1.66 ly/min which was about 0.63 ly/min higher than calculated from observed measurements of radiation. During early morning hours there were no marked differences between the emitted radiation (R_E) derived from the radiation model and observed data.

High values of surface temperature (about 115.5 C, average value for 12 days) were calculated with the radiation model. This indicates a surface temperature without dissipation effects. When compared with the observed temperature in the field, the difference represents the heat lost from the surface to the soil below and the air above.

In the past, many investigators have determined the thermal diffusivity of the soil from soil temperature records using phase and amplitude equations. The investigators who determined thermal diffusivities from annual soil temperature records reported more realistic and consistent values than did those using the daily cycle. In the present study better values were obtained using the phase equation than by use of the amplitude equation.

The equated measurements of the soil profile were determined under dry conditions. For wet conditions, or those where soil water content changes considerably with depth and for more periodic surface temperature change, the phase and amplitude equation cannot be used to determine thermal diffusivity since the thermal properties of soil depend mainly on the mineral composition, the porosity and the soil water content.

The maximum soil temperature at the surface was found to occur between 1300 and 1500 hr. The maximum value of temperature reached at the surface was 71 C. At 2-cm depth, the soil temperature was always warmer than air temperature but the variation of temperature at 10-cm depth approached the air temperature between 2 and 8 m. The minimum temperatures were reached before sunrise; 7.2 C was the minimum value observed in the field.

The variations of temperature at 25-cm depth were found to be 2 to 3 C throughout the day and no notable variations occurred at 50-cm depth.

A computer model was used to predict the temperature of the subsoil from the temperature variation at the soil surface with values of the apparent thermal diffusivity which is dependent upon depth below soil surface and soil temperature. From soil profile temperature data in Figure

3. it is obvious that with the computer model a good estimate can be made of the hourly values of the soil profile. We could note, also, that a better agreement in the profile could be recorded if 5-cm layers were used rather than 10-cm layers.

The maximum transfer of heat occurred in the first two layers of the profile (surface to 10-cm depth). Thirty-three percent of total heat in the profile was concentrated in the first two centimeters of depth, if calculated from daily soil temperature records in the field, and assuming a constant volumetric heat capacity throughout the profile. For estimated values of volumetric heat capacity as reported in Tables 10, 11 and 12, 31% of total value of heat was found in the first layer (0- to 2-cm depth) and almost all the rest of the heat was concentrated in the second layer (2- to 10-cm depth).

Also, for the computed soil temperature, the major heat flow occurred in the first two layers (surface to 10-cm depth), particularly in the first 5 cm (75%). The further decrease occurred gradually with depth.

High values of heat flow were found using temperatures calculated with the radiation model. The difference between these values and the values of heat flow calculated with records of temperature observed in the field indicate the possible loss of heat by conduction and convection.

ACKNOWLEDGMENTS

The author wishes to express his deepest gratitude and thanks to Professor Inge Dirmhirn, Project Leader and thesis director, for her helpful suggestions, advice and interest in this study.

Appreciation is also extended to Dr. R. J. Hanks, Dr. W. L. Pope, graduate students Frank Eaton, Noli Baldazo and David Meyer, and to Charles Craw for their help and suggestions; their aid is deeply appreciated.

Finally, the author wishes to thank his wife, Silvia, for her encouragement and help.

LITERATURE CITED

ANTONOVA, M. A. 1929. Influence of plant and snow cover on soil temperature. Zapiski, Leningradskogo SKhI. Vol. 5. no.5.

AUSTIN, D. D. 1972. The shading effects of plants on soil temperatures in the cold desert. M.S. thesis. Utah State Univ., Logan.

BROWN, E. M. 1943. Seasonal variations in the growth and chemical composition of Kentucky bluegrass. Mo. Agr. Exp. Sta. Res. Bull. 360. 56 pp.

DIKE, P. H. 1958. Thermoelectric thermometry. 3rd ed. Leeds and Northrup Co., Philadelphia. 92 pp.

DIRMHIRN, I. 1972. The radiation environment and the surface temperature on a microscale in the sagebrush desert. US/IBP Desert Biome Research Memo. 72-36. Utah State Univ., Logan. 13 pp.

FLEAGLE, R. G. 1950. Radiation theory of local temperature differences. J. Meteorol. 7:114-120.

GROEN, P. 1947. Note on the theory of nocturnal radiational cooling of the earth's surface. J. Meteorol. 4:63-66.

HANKS, R. J., D. D. AUSTIN, and W. T. ONDRECHEN. 1971. Soil temperature estimation by a numerical method. Soil Sci. Soc. Amer. Proc. 35:665-667.

HANKS, R. J., S. A. BOWERS, and L. D. BARK. 1961. Influence of soil surface conditions on net radiation, soil temperature, and evaporation. Soil Sci. 91:233-238.

HANKS, R. J., and H. S. JACOBS. 1971. Comparison of the calorimetric and flux meter measurements of soil heat flow. Soil Sci. Soc. Amer. Proc. 35:671-674.

HIDE, J. C. 1942. A graphic presentation of temperatures in the surface foot of soil in comparison with air temperatures. Soil Sci. Soc. Amer. Proc. 7:31-35.

HOUGHTON, J. T. 1958. The emissivity of the earth's surface. Quart. J. Roy. Meteorol. Soc. 84:448-450.

HURSH, O. R. 1948. Local climate in the Copper Basin of Tennessee as modified by the removal of vegetation. USDA Circ. 774. 38 pp.

MACK, A. R. 1969. The influence of solar radiation on soil temperatures. Can. J. Plant Sci. 45:203.

MONTEITH, J. L. 1959. The reflection of short-wave radiation by vegetation. Quart. J. Roy. Meteorol. Soc. 85:386-392.

MONTEITH, J. L., and G. SZEICZ. 1961. The radiation balance of bare soil and vegetation. Quart. J. Roy. Meteorol. Soc. 87:159-170.

REEDER, G. 1920. Ground temperatures compared with air temperatures in a shelter. Monthly Weather Rev. 48:637-639.

ROBINSON, G. D. 1947. Notes on the measurement and estimation of atmospheric radiation. Quart. J. Roy. Meteorol. Soc. 73:127-150.

SELLERS, W. D. 1965 Physical climatology. The Univ. of Chicago Press, Chicago. 272 pp.

TAYLOR, E. M. 1928. Soil temperatures in Egypt. J. Agr. Sci. 18:90-122.

WEXLER, H. 1936. Cooling in the lower atmosphere and the structure of polar continental air. Monthly Weather Rev. 64:122-136.

APPENDIX A
Computer Program of Radiation Model

```
COMMON FF(24), ALPHA, BETA, GAMMA, DELTA, EPSLN, TX, TAIR, RA, TSOIL,EZ
COMMON X,DELEP
READ(5, 6)ALPHA, BETA, GAMMA, DELTA, EPSLN
6  FORMAT(3F10.4,E10.4,F10.4)
5  WRITE(6, 7)ALPHA,BETA,GAMMA,DELTA,EPSLN
7  FORMAT(1H1,10X,'PARAMETER VALUES FOR THIS RUN ARE:'/
1 1HO,5x,'ALPHA',6X'BETA',5X,'GAMMA',5X,'DELTA',3x,'EPSILON'/
2 1X,3F10.4E10.4,F10.4///' DATE  HR RS+RD  TAIR(F)  TAIR(K)'
3' E ZERO   RA   RE   T SOIL')
DELEP=DELTA*EPSLN
READ(5, 8)DATE,(FF(I),I=1,24)
8  FORMAT(A6,11F4.1/6X,13F4.1)
DO 9 I=1,24
9  FF(I)=FF(I)/60.0
10  READ(5,11)X1,Y1,Z1,X2,Y2,Z2,X3,Y3,Z3
11  FORMAT(3X,F3.0,F4.0,F8.4/3X,F3.0,F4.0,F8.4/3X,F3.0,F4.0,F8.4)
DIFFY=Y2-Y1
DIFFX=X2-X1
DiffZ=Z2-Z1
SUMX=X1+X2
C=[(Y3-Y2)*DIFFX-DIFFY*(X3-X3)]/[(X3-X2)*DIFFX*(X3-X1)]
B=DIFFY/DIFFX-C*SUMX
A=Y1-(B+C*X1)*X1
CE=[(Z3-Z2)*DIFFX-DIFFZ*(X3-X2)]/[(X3-X2)*DIFFX*(X3-X1)]
BE=DIFFZ/DIFFX-CE*SUMX
AE=Z1-(BE+CE*X1)*X1
X=X1-1.0
TX=A+(B+C*X)*X
EZ=AE+(BE+CE*X)*X
CALL COMPT
WRITE(6,13)DATE,X,FF(X),TX,TAIR,EZ,RA,RE,TSOIL
13  FORMAT(1H,A6,I4,F6.1,2F10.4,F8.3,2F7.2,F8.2)
X=X1
TX=Y1
EZ=Z1
CALL COMPT
WRITE(6,13)DATE,X,FF(X),TX,TAIR,EZ,RA,RE,TSOIL
14  X=X1+1
TX=A+(B+C*X)*X
EZ=AE+(BE+CE*X)*X
CALL COMPT
WRITE(6,13)DATE,X,FF(X),TX,TAIR,EZ,RA,RE,TSOIL
X=X1+2
TX=A+(B+C*X)*X
EZ=AE+(BE+CE*X)*X
CALL COMPT
WRITE(6,13)DATE,X,FF(X),TX,TAIR,EZ,RA,RE,TSOIL
X=X2
TX=Y2
EZ=Z2
CALL COMPT
WRITE(6,13)DATE,X,FF(X),TX,TAIR,EZ,RA,RE,TSOIL
IF(X3.GE.24.0)GO TO 25
X1=X2
Y1=Y2
Z1=Z2
X2=X3
Y2=Y3
Z2=Z3
READ(5,19)X3,Y3,Z3
19  FORMAT(3X,F3.0,F4.0,F8.4
DIFFY=Yx-Y1
DIFFX=X2-X1
DIFFZ=Z2-Z1
SUMX=X1+X2
C=[(Y3-Yx)*DIFFX-DIFFY*(X3-X2)]/[(X3-X2)*DIFFX*(X3-X1)]
B=DIFFY/DIFFX-C*SUMX
CE=[(Z3-Z2)*DIFFX-DIFFZ*(X3-X2)]/[(X3-X2)*DIFFX*(X3-X1)]
BE=DIFFZ/DIFFX-CE*SUMX
AE=Z1-(BE+CE*X1)*X1
GO TO 14
25  X=Z1
DO 30 I=1,3
TX=A+(B+C*X)*X
EZ=AE+(BE+CE*X)*X
CALL COMPT
WRITE(6,13)DATE,X,FF(X),TX,TAIR,EZ,RA,RE,TSOIL
X=X+1
30  CONTINUE
X=X3
TX=Y3
EZ=Z3
CALL COMPT
WRITE(6,13)DATE,X,FF(X),TX,TAIR,EZ,RA,RE,TSOIL
GO TO 5
99  STOP
END

SUBROUTINE COMPT
COMMON FF(24),ALPHA,BETA,GAMMA,DELTA,EPSLN,TX,TAIR,RA,RE,TSOIL,EZ
COMMON X,DELEP
TAIR=(TX-32.0)*5.0/9.0+273.0
RA=DELTA*TAIR**4*[ALPHA-BETA/10.0**(GAMMA*EZ)]
RE=FF(X)*0.84+RA
TSOIL=(RE/DELEP)**0.25
RETURN
END
```

APPENDIX B
Computer Program of Temperature Model

```
DIMENSION B(25),G(25),H(25),E(25),F(25),V(24)
K=16
KK=K+1
READ(5,1) (G(I),I=1,KK
READ(5,1) (B(I),I=1,KK
WRITE(6,5)
WRITE(6,4)(B(I),I=1,KK)
WRITE(6,7)
WRITE(6,4)(G(I),I=1,KKO
WRITE(6,9)
READ(5,1) V
H(1)=V(1)
H(KK)=G(KK)
DELX=10
DELT=1
N=2
AL=0.5
```

```
BT=1.0-AL
POT=DELT/(DELX*DELX)
C--COMPUTATION OF TRIDIAGONAL MATRIX
38 DO 46 I=2,K
BB=BT*POT*(B(I)+B(I-1))+1.0
DD=POT*AL*(B(I-1)*(G(I-1)-G(I))-B(I)*(G(I)-G(I+1)))+G(I)
IF(I.GT.2) GO TO 44
DD=DD+BT*B(I-1)*POT*G(I-1)
F(I)=DD/BB
E(I)=B(I)*BT*POT/BB
GO TO 46
44  IF(I.GE.K) GO TO 47
E(I)=BT*B(I)*POT/(BB-BT*B(I-1)*POT*E(I-1))
F(I)=(DD+BT*B(I-1)*POT*F(I-1))/(BB-BT*B(I-1)*POT*E(I-1))
46 CONTINUE
47  DD=DD+G(I+1)*BT*B(I)*POT
H(I)=(DD+BT*B(I-1)*POT*F(I01))/(BB-BT*B(I-1)*POT*E(Ip1))
48  I=I-1
H(I)=E(I)*H(I+1)+F(I)
IF(I.GT.2)  GO TO 48
CTIME=CTIME+DELT
WRITE(6,2)CTIME,(H(I),I=1,KK)
IF(CTIME.GE.24.0) GO TO 6
H(I)=V(N)
N=N+1
DO 3 I=1,K
3  G(I)=H(I)
GO TO 38
1  FORMAT(14F5.1)
2  FORMAT(25F5.1)
4  FORMAT(5X,25F5.1)
5  FORMAT(45X,1H,'DIFFUSIVITY VALUES')
7  FORMAT(40X,1H,'INITIAL PROFILE TEMPERATURES')
9  FORMAT(48X,1H,'COMPUTED DATA')
6  STOP
END
```

APPENDIX C

Table 19. Data of observed surface and subsoil temperature (in °C) at Curlew Valley (experimental site) on July 7, 1973

Hours	Depth (in cm)					
	0	2	10	25	50	150
0	17.00	23.50	27.00	24.50	19.00	12.50
1	15.25	22.00	26.25	24.50	19.00	12.50
2	14.50	20.75	25.50	24.50	19.00	12.50
3	12.00	19.00	24.75	24.50	19.25	12.50
4	11.75	17.75	24.00	24.25	19.25	12.50
5	9.50	16.50	23.00	24.00	19.25	12.50
6	8.25	15.00	22.50	24.75	19.25	12.50
7	9.50	14.25	21.75	23.50	19.25	12.50
8	18.25	15.50	21.00	23.25	19.25	12.50
9	31.25	21.75	20.75	23.00	19.25	12.50
10	43.00	28.25	21.00	22.75	19.25	12.50
11	53.75	34.25	21.75	22.50	19.25	12.25
12	62.25	40.00	22.75	22.00	19.00	12.25
13	69.50	45.00	24.50	22.00	19.00	12.25
14	69.00	48.50	26.75	22.00	19.00	12.50
15	66.75	49.25	27.25	22.00	19.00	12.25
16	63.75	49.25	29.25	22.50	19.25	12.50
17	58.00	48.00	30.25	23.00	19.25	12.50
18	49.25	45.75	31.00	23.35	19.25	12.50
19	37.75	40.75	31.00	23.75	19.25	12.50
20	24.75	35.50	30.75	24.00	19.25	12.50
21	23.00	31.25	30.00	24.25	19.00	12.50
22	19.25	27.25	29.25	24.50	19.25	12.50
23	17.00	25.00	28.25	24.50	19.25	12.50
24	15.25	23.00	27.25	24.50	19.00	12.50

Table 20. Data of observed surface and subsoil temperature (in °C) at Curlew Valley (experimental site) on July 9, 1973

Hours	Depth (in cm)					
	0	2	10	25	50	150
0	16.75	25.25	28.00	24.50	19.25	12.50
1	14.75	22.75	27.50	24.75	19.50	12.75
2	12.75	20.75	26.50	24.75	19.50	12.75
3	12.25	19.00	25.50	24.75	19.50	12.75
4	10.75	17.75	24.50	24.50	19.00	12.75
5	10.00	16.50	23.75	24.50	19.00	12.75
6	9.25	15.50	23.00	24.25	19.00	12.75
7	8.75	14.50	22.25	24.00	19.00	12.75
8	8.50	14.00	21.50	23.50	19.00	12.75
9	11.25	14.00	21.00	23.50	19.00	12.75
10	21.25	16.25	20.50	23.00	19.00	12.75
11	35.00	23.00	20.25	22.75	19.00	12.75
12	48.00	30.50	20.75	22.50	19.00	12.75
13	55.50	36.50	21.50	22.00	19.25	12.50
14	62.25	42.00	23.00	22.00	19.25	12.50
15	69.25	46.50	24.75	21.75	19.25	12.50
16	71.00	49.75	26.50	21.75	19.25	12.50
17	69.50	51.00	28.25	22.00	19.25	12.50
18	63.50	50.25	29.50	22.25	19.25	12.50
19	57.00	49.00	30.50	22.50	19.25	12.50
20	47.75	45.50	31.00	23.00	19.25	12.50
21	36.50	40.75	31.00	23.25	19.00	12.50
22	29.00	35.50	30.75	23.75	19.00	12.50
23	22.00	31.25	30.25	24.00	19.25	12.75
24	18.00	27.75	29.50	24.50	19.25	12.75

Table 21. Data of observed surface and subsoil temperature (in °C) at Curlew Valley (experimental site) on August 1, 1973

Hours	Depth (in cm)					
	0	2	10	25	50	150
0	12.25	19.25	25.50	23.50	18.75	13.50
1	10.50	18.00	24.75	23.50	18.50	13.50
2	10.00	16.75	24.25	24.00	19.00	14.00
3	8.50	15.75	23.50	24.00	19.25	14.25
4	8.50	14.50	22.50	23.75	19.00	14.25
5	8.25	14.25	21.25	23.25	18.75	14.25
6	7.25	13.50	20.25	23.00	19.00	14.25
7	8.00	12.75	19.75	22.50	18.75	14.25
8	13.25	13.25	18.25	21.25	17.25	13.25
9	25.75	18.50	19.25	22.25	19.20	14.50
10	37.75	24.50	19.50	22.00	19.75	14.50
11	48.00	30.50	20.75	21.75	20.00	14.50
12	53.25	35.50	22.50	21.50	20.50	14.50
13	56.50	38.75	24.25	21.25	20.75	14.25
14	61.50	42.00	26.50	21.25	21.00	14.25
15	62.50	43.75	28.25	21.50	22.00	14.25
16	60.25	44.75	29.75	22.00	22.50	14.25
17	55.75	44.50	31.00	22.50	23.00	14.25
18	46.25	42.00	32.25	23.25	23.75	14.50
19	36.00	38.25	32.25	24.00	23.75	14.50
20	28.75	33.25	32.00	24.25	23.25	14.50
21	22.25	30.25	31.25	24.75	22.50	14.50
22	18.50	26.00	30.00	25.00	22.00	14.50
23	16.50	23.50	28.75	25.25	22.00	14.50
24	15.00	21.75	27.75	25.25	21.75	14.00

APPENDIX D

Table 22. Data of observed global radiation ($R_S + R_D$), net radiation (R_N) and albedo $a(R_S + R_D)$, and calculated net long-wave radiation ($R_A - R_E$) in ly/min at Curlew Valley (experimental site) on July 7, 1973

Hours	$R_S + R_D$	R_N	$(R_S + R_D)a$	$R_A - R_E$
1		-0.1340		-0.1340
2		-0.2305		-0.1205
3		-0.1195		-0.1195
4		-0.1270		-0.1270
5	0.0648	-0.0750	0.0104	-0.1294
6	0.3015	0.1150	0.0480	-0.1370
7	0.5703	0.3290	0.0912	-0.1200
8	0.8185	0.5090	0.1309	-0.1800
9	1.0611	0.6714	0.1697	-0.2200
10	1.2446	0.7955	0.1991	-0.2500
11	1.3513	0.8700	0.2162	-0.2651
12	1.3874	0.8800	0.2219	-0.2800
13	1.3550	0.8650	0.2168	-0.2700
14	1.2426	0.8150	0.1988	-0.2300
15	1.0591	0.7116	0.1694	-0.2100
16	0.8249	0.5130	0.1319	-0.1800
17	0.5575	0.3180	0.0892	-0.1500
18	0.2902	0.1238	0.0464	-0.1200
19	0.0600	-0.0790	0.0006	-0.1300
20		-0.1200		-0.1200
21		-0.1200		-0.1200
22		-0.1160		-0.1160

Table 23. Data of observed global radiation ($R_S + R_D$), net radiation (R_N) and albedo $a(R_S + R_D)$, and calculated net long-wave radiation ($R_A - R_E$) in ly/min at Curlew Valley (experimental site) on July 9, 1973

Hours	$R_S + R_D$	R_N	$(R_S + R_D)a$	$R_A - R_E$
1		-0.0970		-0.0970
2		-0.0935		-0.0935
3		-0.0925		-0.0925
4		-0.0880		-0.0880
5	0.0844	-0.0240	0.0135	-0.0949
6	0.2965	0.1530	0.0470	-0.0961
7	0.5689	0.3479	0.0910	-0.1300
8	0.8344	0.5309	0.1335	-0.1700
9	1.0655	0.6950	0.1705	-0.2000
10	1.2382	0.8073	0.1981	-0.2328
11	1.3487	0.8480	0.2157	-0.2850
12	1.3861	0.8532	0.2217	-0.3112
13	1.3379	0.8314	0.2140	-0.2925
14	1.2123	0.7664	0.1939	-0.2520
15	1.0242	0.6504	0.1638	-0.2100
16	0.7900	0.5036	0.1264	-0.1600
17	0.5100	0.3084	0.0816	-0.1200
18	0.2700	0.1370	0.0430	-0.0900
19	0.0350	-0.0566	0.0056	-0.0860
20		-0.1131		-0.1131
21		-0.1033		-0.1033

Table 24. Data of observed global radiation ($R_S + R_D$), net radiation (R_N) and albedo $a(R_S + R_D)$, and calculated net long-wave radiation ($R_A - R_E$) in ly/min at Curlew Valley (experimental site) on August 1, 1973

Hours	$R_S + R_D$	R_N	$(R_S + R_D)a$	$R_A - R_E$
1		-0.0980		-0.0980
2		-0.0900		-0.0900
3		-0.0954		-0.0954
4		-0.0954		-0.0954
5	0.0627	-0.0588	0.0100	-0.1115
6	0.2533	0.0899	0.0405	-0.1229
7	0.5400	0.3430	0.0864	-0.1133
8	0.7927	0.5159	0.1268	-0.1500
9	1.0276	0.6727	0.1644	-0.1900
10	1.2054	0.7934	0.1928	-0.2192
11	1.3087	0.8700	0.2093	-0.2294
12	1.3419	0.87245	0.2147	-0.25475
13	1.3106	0.8314	0.2096	-0.2696
14	1.2036	0.74255	0.1925	-0.26605
15	1.0246	0.63375	0.1639	-0.2269
16	0.7976	0.4908	0.2376	-0.1792
17	0.5399	0.2999	0.0860	-0.1540
18	0.2700	0.0722	0.0432	-0.1546
19	0.0500	-0.0986	0.0080	-0.1406
20		-0.1298		-0.1298
21		-0.1127		-0.1127
22		-0.1099		-0.1099

APPENDIX E

Table 25. Data of observed air temperature (in °C) at Curlew Valley (experimental site) on July 7, 1973

Hours	Height (in cm)							
	800	400	200	100	50	20	5	5(shade)
1	19.25	19.00	18.25	8.00	-1.25	17.50	17.75	17.00
2	19.00	18.00	16.50	6.50	-3.25	14.75	14.25	14.50
3	16.25	15.75	14.25	5.50	-4.50	14.00	11.00	11.75
4	14.75	14.50	14.00	5.00	-3.50	12.75	12.50	12.75
5	13.25	12.00	10.75	2.00	-6.00	9.00	8.75	8.50
6	12.50	10.25	10.00	0.50	-6.25	8.50	8.25	7.50
7	11.25	11.00	10.00	1.75	-3.50	11.50	11.00	10.75
8	17.50	17.50	17.50	8.00	-0.25	18.75	18.50	18.75
9	21.25	21.00	21.50	10.75	1.75	23.50	23.00	24.00
10	23.50	24.50	26.00	26.75	1.75	28.00	29.50	28.75
11	25.00	25.00	25.25	27.50	5.25	32.25	33.50	34.00
12	27.25	27.00	27.00	16.00	5.50	30.00	36.50	32.00
13	30.00	30.25	30.00	18.00	5.75	30.75	39.75	34.50
14	30.50	30.75	30.50	17.00	6.50	32.75	39.00	39.00
15	30.75	33.00	34.00	21.75	7.75	36.50	37.75	38.25
16	31.00	34.00	34.75	20.50	6.50	38.25	39.25	39.50
17	32.00	32.50	33.50	20.50	6.75	37.25	36.75	38.25
18	33.50	33.25	32.75	20.00	6.25	36.50	33.75	37.25
19	32.25	32.25	32.50	19.75	5.75	34.00	34.50	34.75
20	31.50	32.00	32.00	19.00	5.25	33.00	31.25	31.75
21	28.75	28.00	27.25	13.75	1.75	20.50	19.75	20.25
22	21.75	20.75	20.00	9.00	-1.25	19.00	18.50	21.75
23	21.50	21.00	19.50	8.50	-2.75	15.25	14.25	14.25
24	19.75	17.25	16.00	8.75	-0.50	14.75	14.75	14.25